54 Campbell, I. K., O'Donnell, K., Lawlor, K. E. and Wicks, I. P. 2001. Severe inflammatory arthritis and lymphadenopathy in the absence of TNF. *J. Clin. Invest.* 107:1519.
55 Tada, Y., Ho, A., Koarada, S. *et al.* 2001. Collagen-induced arthritis in TNF receptor-1-deficient mice: TNF receptor-2 can modulate arthritis in the absence of TNF receptor-1. *Clin. Immunol.* 99:325.
56 Mori, L., Iselin, S., De Libero, G. and Lesslauer, W. 1996. Attenuation of collagen-induced arthritis in 55-kDa TNF receptor type 1 (TNFR1)-IgG1-treated and TNFR1-deficient mice. *J. Immunol.* 157:3178.
57 Huang, D., Tani, M., Wang, J. *et al.* 2002. Pertussis toxin-induced reversible encephalopathy dependent on monocyte chemoattractant protein-1 overexpression in mice. *J. Neurosci.* 22:10633.
58 Rand, M. L., Warren, J. S., Mansour, M. K., Newman, W. and Ringler, D. J. 1996. Inhibition of T cell recruitment and cutaneous delayed-type hypersensitivity-induced inflammation with antibodies to monocyte chemoattractant protein-1. *Am. J. Pathol.* 148:855.
59 Kawakami, K., Koguchi, Y., Qureshi, M. H. *et al.* 2000. Reduced host resistance and Th1 response to *Cryptococcus neoformans* in interleukin-18 deficient mice. *FEMS Microbiol. Lett.* 186:121.
60 Cruikshank, W. W., Kornfeld, H. and Center, D. M. 2000. Interleukin-16. *J. Leukoc. Biol.* 67:757.
61 Wilkinson, R. J., Patel, P., Llewelyn, M. *et al.* 1999. Influence of polymorphism in the genes for the interleukin (IL)-1 receptor antagonist and IL-1beta on tuberculosis. *J. Exp. Med.* 189:1863.

mediated by complement bypass systems. Fourth, and probably most important, the type of assay represents the wave of the future in detecting the activity of the complement system in human disease. As these more informative detection systems (like the one used in this report) come into routine clinical use, other examples of these bypass type pathways will likely be uncovered. For human diseases, these more specific and quantitative assay systems will establish which pathway of complement activation is playing a role in disease and elucidate which one to modulate with therapeutic agents.

Finally, a word of caution is in order. These bypass pathways are often not considered by investigators attempting to define the role of the complement system in disease states. For example, C4-deficient animals are widely used to rule out a contribution of the classical pathway and/or lectin pathway in mouse models of human disease. One must be wary of such interpretations in view of bypass cascades that become operative in "deficient" states. Thus the natural maturation of an antibody response to an infectious organism (i.e., to go rapidly into antibody excess) is all that is necessary to trigger these more ancient bypass pathways. Using our current methods, such pathways are not analyzed in clinical medicine or in animal models of human disease.

Address correspondence to: John P. Atkinson, Washington University School of Medicine, 660 South Euclid Avenue, Box 8045, St. Louis, Missouri 63110, USA. Phone: (314) 362-8391; Fax: (314) 362-1366; E-mail: jatkinso@im.wustl.edu.

1. May, J.E., and Frank, M.M. 1973. A new complement-mediated cytolytic mechanism-the C1-bypass activation pathway. *Proc. Natl. Acad. Sci. U. S. A.* **70**:649-652.
2. May, J.E., and Frank, M.M. 1973. Hemolysis of sheep erythrocytes in guinea pig serum deficient in the fourth component of complement. I. Antibody and serum requirements. *J. Immunol.* **111**:1661-1667.
3. May, J.E., and Frank, M.M. 1973. Hemolysis of sheep erythrocytes in guinea pig serum deficient in the fourth component of complement. II. Evidence for involvement of C1 and components of the alternate complement pathway. *J. Immunol.* **111**:1668-1676.
4. Matsushita, M., and Okada, H. 1986. Alternative complement pathway activation by C4b deposited during classical pathway activation. *J. Immunol.* **136**:2994-2998.
5. Farries, T.C., Knutzen Steuer, K.L., and Atkinson, J.P. 1990. The mechanism of activation of the alternative pathway of complement by cell-bound C4b. *Mol. Immunol.* **27**:1155-1161.
6. Knutzen-Steuer, K.L., et al. 1989. Lysis of sensitized sheep erythrocytes in human sera deficient in the second component of complement. *J. Immunol.* **143**:2256-2261.
7. Selander, B., et al. 2006. Mannan-binding lectin activates C3 and the alternative complement pathway without involvement of C2. *J. Clin. Invest.* **116**:1425-1434. doi:10.1172/JCI25982.
8. Seelen, M.A., et al. 2005. Functional analysis of the classical, alternative, and MBL pathways of the complement system: standardization and validation of a simple ELISA. *J. Immunol. Methods.* **296**:187-198.
9. Deguchi, M., Gillin, F.D., and Gigli, I. 1987. Mechanism of killing of *Giardia lamblia* trophozoites by complement. *J. Clin. Invest.* **79**:1296-1302.
10. Wagner, E., Platt, J.L., Howell, D.N., Marsh, H.C., Jr., and Frank, M.M. 1999. IgG and complement-mediated tissue damage in the absence of C2: evidence of a functionally active C2-bypass pathway in a guinea pig model. *J. Immunol.* **163**:3549-3558.
11. Traustadottir, K.H., Rafnar, B.O., Steinsson, K., Valdimarsson, H., and Erlendsson, K. 1998. Participation of factor B in residual immune complex red cell binding activity observed in serum from a C2-deficient systemic lupus erythematosus patient may delay the appearance of clinical symptoms. *Arthritis Rheum.* **41**:427-434.
12. Klint, C., Gullstrand, B., Sturfelt, G., and Truedsson, L. 2000. Binding of immune complexes to erythrocyte CR1 (CD35): difference in requirement of classical pathway components and indication of alternative pathway-mediated binding in C2-deficiency. *Scand. J. Immunol.* **52**:103-108.
13. Nolin, L., et al. 1979. Possible C1q bypass loop activation in the haemolytic uraemic syndrome. *Clin. Exp. Immunol.* **35**:107-111.

The IL-23/IL-17 axis in inflammation

Yoichiro Iwakura and Harumichi Ishigame

Center for Experimental Medicine, Institute of Medical Science, University of Tokyo, Tokyo, Japan.

IL-23 induces the differentiation of naive CD4+ T cells into highly pathogenic helper T cells (Th17/Th$_{IL-17}$) that produce IL-17, IL-17F, IL-6, and TNF-α, but not IFN-γ and IL-4. Two studies in this issue of the *JCI* demonstrate that blocking IL-23 or its downstream factors IL-17 and IL-6, but not the IL-12/IFN-γ pathways, can significantly suppress disease development in animal models of inflammatory bowel disease and MS (see the related articles beginning on pages 1310 and 1317). These studies suggest that the IL-23/IL-17 pathway may be a novel therapeutic target for the treatment of chronic inflammatory diseases.

Th17/Th$_{IL-17}$ is a new CD4+ helper T cell subset that produces IL-17

Upon antigenic stimulation, naive CD4+ T cells differentiate into 2 subsets, Th1 and Th2 cells, characterized by different cytokine production profiles and effector functions (Figure 1). Th1 cells produce large quantities of IFN-γ and mediate cellular immunity while Th2 cells, which are involved in humoral immunity, primarily produce IL-4, IL-5, and IL-13. IL-12, a heterodimer of the p40 and p35 subunits, induces the differentiation of naive CD4+ T cells into IFN-γ-producing Th1 cells through activation of STAT4. IFN-γ signals are transduced by STAT1, which activates a downstream transcription factor, T-bet, that enhances the expression of genes specific to Th1 cells. In contrast, IL-4 induces STAT6 activation, promoting the expression of GATA-3, a transcriptional factor essential for both IL-4 production and Th2 cell differentiation. Recently, it was reported that CD4+ T cells isolated from the inflamed joints of patients with Lyme disease contain a subset of IL-17-producing CD4+ T cells that are distinct from those producing either IL-4 or IFN-γ (Figure 1) (1). These IL-17-producing CD4+ T cells were dubbed Th17 or Th$_{IL-17}$ cells (2-4).

IL-17, a proinflammatory cytokine predominantly produced by activated T cells, enhances T cell priming and stimulates fibroblasts, endothelial cells, macrophages, and epithelial cells to produce multiple proinflammatory mediators, including IL-1, IL-6, TNF-α, NOS-2, metalloproteases, and chemokines, resulting in the induction of inflammation (5, 6). IL-17 expression is increased in patients with a variety of allergic and autoimmune diseases, such as RA, MS, inflamma-

Nonstandard abbreviations used: CIA, collagen-induced arthritis; IBD, inflammatory bowel disease; IL-1Ra, IL-1 receptor antagonist; R, receptor.

Conflict of interest: The authors have declared that no conflict of interest exists.

Citation for this article: *J. Clin. Invest.* **116**:1218-1222 (2006). doi:10.1172/JCI28508.

162

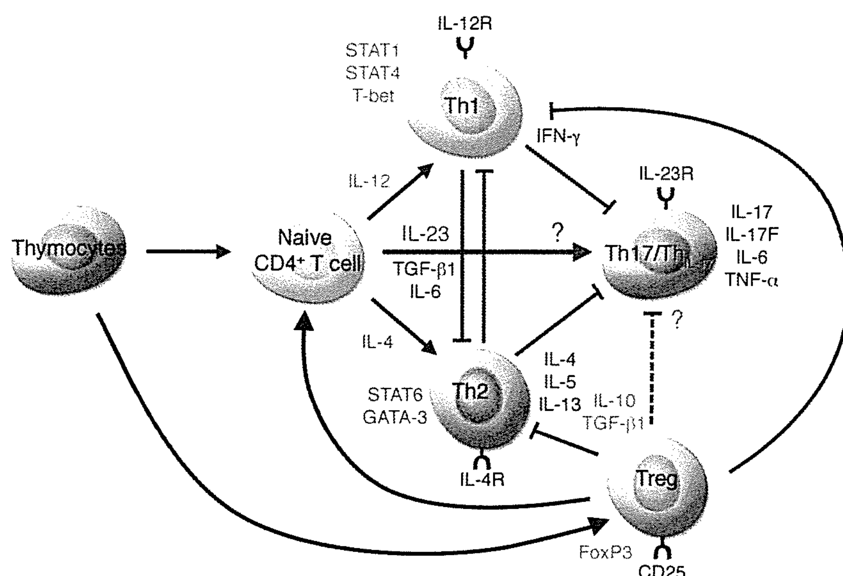

Figure 1
IL-23 promotes the development of an IL-17–producing CD4+ helper T cell subset. IL-23 induces the differentiation of naive CD4+ T cells into IL-17–producing helper T cells (Th17/Th$_{IL-17}$) via mechanisms that are distinct from the Th1 and Th2 differentiation pathways. The transcriptional factors critical for the development of Th1 (STAT1, STAT4, and T-bet) and Th2 (STAT6) cells are not required for the induction of Th17/Th$_{IL-17}$ cells. The transcriptional factor(s) essential for the development of Th17/Th$_{IL-17}$ cells remain unknown. IFN-γ and IL-4 antagonize each other in the differentiation of Th1 and Th2 cells and the promotion of their function. IFN-γ also suppresses the differentiation of Th17/Th$_{IL-17}$ cells by reducing IL-23R expression on CD4+ T cells. IL-4 also inhibits the development of Th17/Th$_{IL-17}$ cells. It is not known, however, whether Th17/Th$_{IL-17}$ cells inhibit the development of Th1 and Th2 cells. Tregs, an immune-modulating subset of CD4+ T cells, suppress the differentiation and effector function of Th1 and Th2 cells. Recent studies suggest that Treg-derived TGF-β induces the differentiation of Th17/Th$_{IL-17}$ cells from naive CD4+ T cells in the presence of IL-6 in vitro (26). However, the precise effect(s) of Tregs on Th17/Th$_{IL-17}$ cells are as yet unknown.

tory bowel disease (IBD), and asthma, suggesting the contribution of IL-17 to the induction and/or development of such diseases. Supporting this, the involvement of this cytokine in such responses is demonstrated in animal models; autoimmune disorders such as collagen-induced arthritis (CIA) and EAE, animal models for RA and MS, respectively, as well as allergic responses such as contact hypersensitivity, delayed-type hypersensitivity, and airway hypersensitivity were suppressed in IL-17-deficient (IL-17$^{-/-}$) mice (7, 8) (Y. Komiyama et al., University of Tokyo, Tokyo, Japan, unpublished observations). Therefore, Th17/Th$_{IL-17}$ cells are likely to play critical roles in the development of autoimmunity and allergic reactions.

The IL-23/IL-17, but not IL-12/IFN-γ, axis is critical for the development of autoimmune inflammatory diseases

The development of autoimmune diseases, such as RA, MS, and IBD, is thought to be mediated by Th1 cells because high levels of IL-12 and IFN-γ are detected in inflammatory sites (9). In addition, treatment with mAbs against IL-12p40 suppresses such disease development in humans and animal disease models (9, 10). However, mice deficient in IL-12p35, IL-12 receptor β2 (IL-12Rβ2), IFN-γ, IFN-γR, or STAT1, which are critical molecules in IL-12/IFN-γ–mediated responses, exhibit an increased severity of diseases such as EAE and CIA (11-13). These observations are inconsistent with the notion that IL-12 is responsible for such disease development. As IL-23, an IL-12 family cytokine consisting of the p19 and p40 subunits, shares the p40 subunit with IL-12 and anti-p40 mAbs inhibit both cytokines, the involvement of IL-23 is suggested. Current evidence suggests that IL-23 is responsible for the differentiation and expansion of Th17/Th$_{IL-17}$ cells from naive CD4+ T cells (2, 4, 14).

In this issue of the *JCI*, Yen et al. report on their use of IL-23p19$^{-/-}$ and IL-12p35$^{-/-}$ mice to demonstrate that IL-23, but not IL-12, is essential for the development of intestinal inflammation (15). They used IL-10$^{-/-}$ mice as a model of T cell–mediated IBD (16) and showed that the development of colitis was greatly suppressed by IL-23p19 deficiency but not IL-12p35 deficiency. Exogenous IL-23 administration accelerated the onset of colitis in Rag$^{-/-}$ mice engrafted with IL-10$^{-/-}$CD4+ T cells. Notably, IL-17 production was abolished in IL-23p19$^{-/-}$ mice while IFN-γ and IL-4 production were unaffected. IL-17 and IL-6 expression by anti-CD3 mAb–stimulated memory CD4+ T cells were augmented by IL-23, but not by IL-12, indicating that IL-23 can simulate memory CD4+ T cells. This result contrasts with the ability of IL-12 to stimulate naive CD4+ T cells. Moreover, treatment with both anti–IL-6 and anti–IL-17 mAbs significantly ameliorated the severity of the intestinal inflammation induced by IL-23–treated Rag$^{-/-}$ mice engrafted with IL-10$^{-/-}$CD4+CD45RB^{hi} T cells. These observations suggest that IL-17 and IL-6 derived from memory T cells are responsible for the development of intestinal inflammation downstream of IL-23.

Also in this issue of the *JCI*, Chen et al. report on their use of newly developed anti–IL-23p19 mAbs to demonstrate the involvement of IL-23 in EAE (17). The authors previously demonstrated that IL-23p19$^{-/-}$ mice are resistant to EAE and CIA; production of IL-17, but not IFN-γ, is almost completely abolished in these mutant mice (3, 18, 19). In contrast, IL-23p35$^{-/-}$ mice exhibited decreased IFN-γ production and increased IL-17 production, suggesting that IFN-γ may suppress IL-17 production. Furthermore, IL-23–induced but not IL-12–induced proteolipid protein peptide–specific T cells are highly encephalogenic (3). Consistent with these reports, the development of EAE was efficiently suppressed by treatment with anti–IL-23p19 or anti–IL-12/IL-23p40 mAbs by inhibiting infiltration of IL-17–, IFN-γ–, and TNF-α–producing CD4+ T cells in the CNS. Disease severity correlated well with serum IL-17 levels; treatment with anti–IL-17 mAbs ameliorated the clinical disease score. Meanwhile, treatment with anti–IFN-γ mAbs exacerbated disease, consistent with previous observations that IFN-γ$^{-/-}$ and IFN-γR$^{-/-}$ mice are highly susceptible to EAE (12, 13). Thus, it is clearly shown that the IL-23/IL-17 pathway, rather than the IL-12/IFN-γ pathway, is critical for the development of autoimmune diseases.

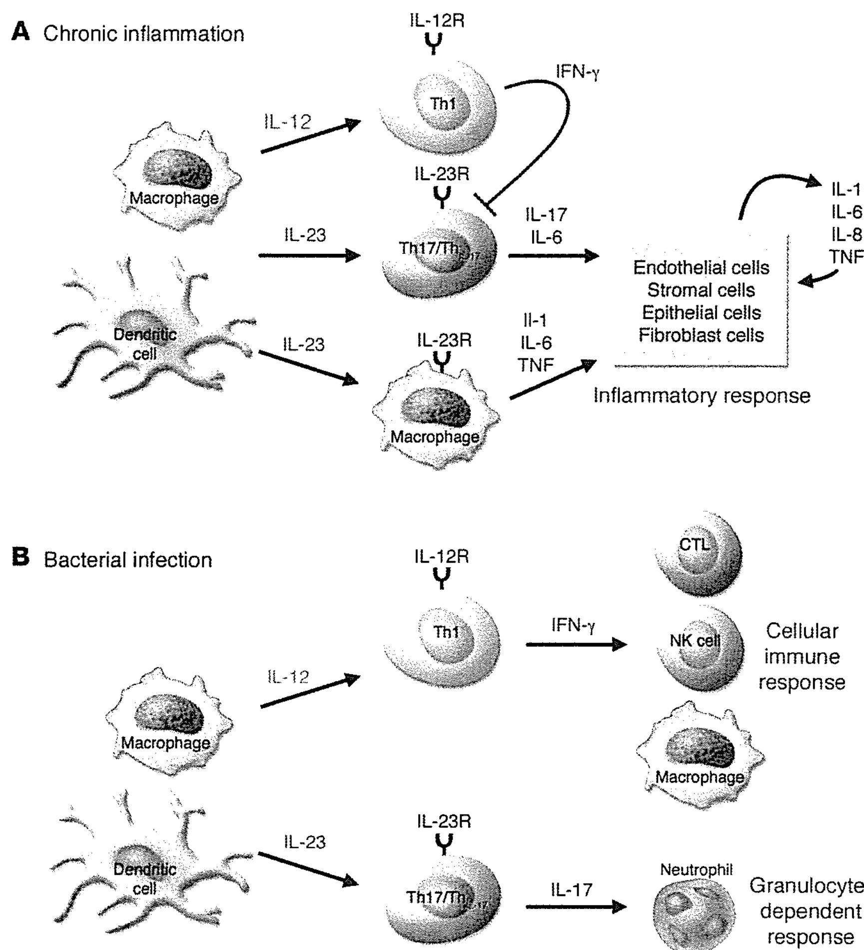

Figure 2
The role of the IL-23/IL-17 axis in inflammation and infection. The IL-23/IL-17 axis plays an important role in the development of chronic inflammation and in host defenses against bacterial infection. (**A**) In chronic inflammation, antigen-stimulated dendritic cells and macrophages produce IL-23, which promotes the development of Th17/Th$_{IL-17}$ cells. Th17/Th$_{IL-17}$ cells produce IL-17, which enhances T cell priming and triggers potent inflammatory responses by inducing the production of a variety of inflammatory mediators. IL-23 also acts on dendritic cells and macrophages in an autocrine/paracrine manner to stimulate the generation of proinflammatory cytokines, such as IL-1, IL-6, and TNF-α. IL-12–stimulated Th1 cells produce IFN-γ and suppress the differentiation of Th17/Th$_{IL-17}$ cells. Th1 cells may play an immunoregulatory, not a pathogenic, role in the development of chronic inflammation. (**B**) Upon bacterial infection, IL-23 is rapidly produced by activated macrophages and dendritic cells at the site of infection. IL-23 then activates local resident Th17/Th$_{IL-17}$ cells and other IL-17–producing cells, such as CD8$^+$ T cells and γδ T cells. Production of IL-17 by these cells induces G-CSF production from stromal cells. The IL-23/IL-17/G-CSF pathway augments neutrophil recruitment to the infection site, contributing to extracellular bacterial clearance. IL-23 also increases the production of IL-1, IL-6, and TNF-α in an autocrine/paracrine manner. In contrast, Th1 cells produce IFN-γ and stimulate CD8$^+$ cytotoxic T lympocytes, NK cells, and macrophages. IFN-γ enhances antigen presentation by inducing expression of MHC molecules and activates cells to produce cytolytic molecules, including perforin and granzyme, which promote the elimination of intracellular bacteria.

IL-23 causes inflammation through IL-17–dependent and IL-17–independent pathways

Anti-IL-17 treatment did not prevent the onset and relapse of EAE with the same efficiency as anti-IL-23p19 or anti-IL-12/IL-23p40 treatment, suggesting that the effects of IL-23 cannot be explained by the action of IL-17 alone. We also observed that EAE progression is only partially suppressed even in IL-17$^{-/-}$ mice, suggesting the involvement of additional factors (Komiyama et al., unpublished observations). The transcription factor T-bet is responsible for enhancing IFN-γ production and increasing IL-12Rβ2 expression (20). In contrast to IFN-γ$^{-/-}$ mice, T-bet$^{-/-}$ mice are highly resistant to EAE development (11). As Th17/Th$_{IL-17}$ cells were present in T-bet$^{-/-}$ mice, Chen et al. suggested that Th17/Th$_{IL-17}$ cells are not sufficient to induce disease and that additional T-bet–dependent factors and/or cell populations play significant roles in disease pathogenesis (17). With respect to this, T-bet expression on dendritic cells, but not on T cells, is required for IL-1 and chemokine production, contributing to the development of collagen antibody–induced arthritis (21). In the current studies, Chen et al. (17) suggested that IL-23 may directly activate a subset of macrophages and dendritic cells expressing IL-23R, resulting in the production of inflammatory mediators, such as TNF-α and IL-1 (18, 22). However, as progression of diseases such as EAE and CIA is only minimally affected in TNF-α$^{-/-}$ mice and anti-TNF-α treatment of wild-type mice results in more severe MS (23), TNF-α is not critical for the development of this disease. In contrast, IL-6$^{-/-}$ and IL-1$^{-/-}$ mice are significantly resistant, and IL-1 receptor antagonist–deficient (IL-1Ra$^{-/-}$) mice are more susceptible to EAE (24, 25). Thus, IL-6 and IL-1 likely play important roles in the development of this disease. These observations suggest that IL-23 can induce chronic inflammation through 2 independent pathways: (a) activation of Th17/Th$_{IL-17}$ cells; and (b) induction of IL-1 and IL-6 production via myeloid cell activation (Figure 2).

Additional IL-17 family molecules may also play an important role in the development of inflammatory diseases. The IL-17 family currently consists of 6 family members; some of these family members, such as IL-17F, share significant amino acid homology with IL-17 (also known as IL-17A), are induced by IL-23, bind the same receptor as IL-17, and are produced by Th17/Th$_{IL-17}$ cells. Thus, it is possible that these additional IL-17 members may be involved in inflammatory responses. It is important to elucidate the functions of these IL-17 family molecules in normal physiology and in disease pathogenesis.

The Th17/Th$_{IL-17}$ differentiation mechanism is not yet known

Naive CD4$^+$ T cells isolated from mice deficient in STAT1, STAT4, or T-bet

retained the ability to differentiate into Th17/Th_{IL-17} cells in vitro following TCR stimulation in the presence of IL-23 (2). The generation of Th17/Th_{IL-17} cells following immunization with antigen stimulation was also normal in mice deficient for STAT4, STAT6, or T-bet (4). Thus, these Th1- and Th2-specific transcriptional factors are not involved in the differentiation of Th17/Th_{IL-17} cells, indicating that the Th17/Th_{IL-17} lineage is independent from these classical Th cell lineages. In this issue, Chen et al. (17) demonstrate that T-bet$^{-/-}$ lymph node cells produced IL-17 upon stimulation with anti-CD3 mAbs, consistent with previous reports (2, 4). Exogenous IL-23, however, did not further enhance IL-17 production in T-bet$^{-/-}$ lymph node cells, suggesting that T-bet may influence IL-23 responsiveness during early Th17/Th_{IL-17} development (17). Thus, the transcriptional factors involved in Th17/Th_{IL-17} cell development still remain to be elucidated (Figure 1). With regard to this, STAT3 was recently implicated in the IL-23R signaling pathway (22).

As IL-12Rβ1, the common subunit of IL-12R and IL-23R, is constitutively expressed in naive CD4$^+$ T cells, IL-12Rβ2 and IL-23R expression are critical for the responsiveness to IL-12 and IL-23 and development of Th1 and Th17/Th_{IL-17} cell lineages. Only memory and/or activated T cells express IL-23R; naive Th17/Th_{IL-17} progenitor cells are devoid of this molecule (22). However, when naive CD4$^+$ T cells were stimulated with IL-23 in the presence of anti-IL-4 and anti-IFN-γ mAbs, a large IL-17-producing population was observed, indicating that IFN-γ and IL-4 inhibit the differentiation of Th17/Th_{IL-17} cells from naive CD4$^+$ T cells. IFN-γ and STAT1 signaling inhibit the differentiation by downregulating the expression of IL-23R (2). Although IL-4 also inhibits Th17 cell expansion, the mechanism governing this suppression is not known (2, 4). Thus, the identification of the signals that induce IL-23R expression on naive CD4$^+$ T cells is crucial in elucidating the mechanisms of Th17/Th_{IL-17} cell lineage differentiation.

Recently, Veldhoen et al. reported that Treg-derived TGF-β induces the differentiation of Th17/Th_{IL-17} cells from naive CD4$^+$ T cells in the presence of IL-6 in vitro (Figure 1) (26). TGF-β–mediated Th17/Th_{IL-17} cell differentiation is promoted by dendritic cell–derived IL-1β and TNF-α. They showed that IL-23 is not essential for the development of Th17/Th_{IL-17} cells, but required for their survival and expansion through the positive feedback loop that upregulates IL-6, IL-1β, and TNF-α. Thus, current evidence provides us with 2 Th17/Th_{IL-17} cell differentiation pathways; one is IL-23 dependent and the other is IL-23 independent. Further studies are definitely required to address the precise roles of IL-23 and other factors in the development of Th17/Th_{IL-17} cells in vivo.

Concluding remarks

While the importance of IL-12 in host defense against bacteria is widely accepted, the role of IL-23 in host defense is not well understood (Figure 2). Recent studies have revealed that IL-12 and IL-23 have different roles in host defense. Mice deficient in IFN-γ, IFN-γR, or STAT1 are highly susceptible to many different pathogens, including *Leishmania major*, *Listeria monocytogenes*, and *Mycobacterium tuberculosis* (27). IL-23 and IL-17 are also important in host defenses against infection. It should be noted that IL-12/IFN-γ are primarily involved in host defenses against intracellular pathogens while IL-23/IL-17 are important for defenses against extracellular pathogens, including *Klebsiella pneumoniae* (28). This is because IFN-γ stimulates the immune system to kill intracellular bacteria and infected host cells while IL-17 recruits and activates neutrophils. The detailed host defense mechanisms involving IL-23 and IL-17, however, still remain to be elucidated.

IL-17 is produced not only by Th17/Th_{IL-17} cells, but also by activated CD8$^+$ T cells, TCRγδ$^+$ T cells, and neutrophils (5, 29). We have observed that CD4$^-$CD8$^-$TCRγδ$^+$ T cells also produce IL-17 in IL-1Ra$^{-/-}$ mice, which spontaneously develop autoimmune arthritis (Komiyama et al., unpublished observations). Development of arthritis in these mice can be completely suppressed by IL-17 deficiency (6). Thus, IL-17 production by cells distinct from Th17/Th_{IL-17} cells may also be involved in inflammatory responses and host defense mechanisms. It remains unclear, however, which of these producer cells are involved in the different allergic and infectious diseases and how the differentiation pathways of these cell lineages are controlled.

Taken together, accumulating evidence suggests that 3 independent pathways are involved in inflammatory responses: IL-12/IFN-γ, IL-4/IL-5/IL-13, and IL-23/IL-17. These pathways are largely exclusive, although the effect of Th17/Th_{IL-17} cells on Th1 and Th2 cells is not well understood. Identification of the major immune pathways responsible for the development of each disease is important for its treatment because suppression of 1 pathway may accelerate the others. Therapeutic targeting of the newly discovered IL-23/IL-17 immune axis may prove effective for the treatment of autoimmune and allergic inflammatory responses.

165

Acknowledgments

We would like to thank Shigeru Kakuta and Susumu Nakae (Stanford University School of Medicine, Stanford, California, USA) for critical reading of the manuscript.

Address correspondence to: Yoichiro Iwakura, Center for Experimental Medicine, Institute of Medical Science, University of Tokyo, 4-6-1 Shirokanedai, Minato-ku, Tokyo 108-8639, Japan. Phone: 81-3-5449-5536; Fax: 81-3-5449-5430; E-mail: iwakura@ims.u-tokyo.ac.jp.

1. Infante-Duarte, C., Horton, H.F., Byrne, M.C., and Kamradt, T. 2000. Microbial lipopeptides induce the production of IL-17 in Th cells. *J. Immunol.* **165**:6107–6115.
2. Harrington, L.E., et al. 2005. Interleukin 17-producing CD4+ effector T cells develop via a lineage distinct from the T helper type 1 and 2 lineages. *Nat. Immunol.* **6**:1123–1132.
3. Langrish, C.L., et al. 2005. IL-23 drives a pathogenic T cell population that induces autoimmune inflammation. *J. Exp. Med.* **201**:233–240.
4. Park, H., et al. 2005. A distinct lineage of CD4 T cells regulates tissue inflammation by producing interleukin 17. *Nat. Immunol.* **6**:1133–1141.
5. Kolls, J.K., and Linden, A. 2004. Interleukin-17 family members and inflammation. *Immunity.* **21**:467–476.
6. Nakae, S., et al. 2003. IL-17 production from activated T cells is required for the spontaneous development of destructive arthritis in mice deficient in IL-1 receptor antagonist. *Proc. Natl. Acad. Sci. U. S. A.* **100**:5986–5990.
7. Nakae, S., et al. 2002. Antigen-specific T cell sensitization is impaired in IL-17-deficient mice, causing suppression of allergic cellular and humoral responses. *Immunity.* **17**:375–387.
8. Nakae, S., Nambu, A., Sudo, K., and Iwakura, Y. 2003. Suppression of immune induction of collagen-induced arthritis in IL-17-deficient mice. *J. Immunol.* **171**:6173–6177.
9. Gately, M.K., et al. 1998. The interleukin-12/interleukin-12-receptor system: role in normal and pathologic immune responses. *Annu. Rev. Immunol.* **16**:495–521.
10. Mannon, P.J., et al. 2004. Anti-interleukin-12 antibody for active Crohn's disease. *N. Engl. J. Med.* **351**:2069–2079.
11. Bettelli, E., et al. 2004. Loss of T-bet, but not STAT1, prevents the development of experimental autoimmune encephalomyelitis. *J. Exp. Med.* **200**:79–87.

12. Hunter, C.A. 2005. New IL-12-family members: IL-23 and IL-27, cytokines with divergent functions. *Nat. Rev. Immunol.* **5**:521–531.
13. McKenzie, B.S., Kastelein, R.A., and Cua, D.J. 2006. Understanding the IL-23-IL-17 immune pathway. *Trends Immunol.* **27**:17–23.
14. Aggarwal, S., Ghilardi, N., Xie, M.H., de Sauvage, F.J., and Gurney, A.L. 2003. Interleukin-23 promotes a distinct CD4 T cell activation state characterized by the production of interleukin-17. *J. Biol. Chem.* **278**:1910–1914.
15. Yen, D., et al. 2006. IL-23 is essential for T cell-mediated colitis and promotes inflammation via IL-17 and IL-6. *J. Clin. Invest.* **116**:1310–1316. doi:10.1172/JCI21404.
16. Strober, W., Fuss, I.J., and Blumberg, R.S. 2002. The immunology of mucosal models of inflammation. *Annu. Rev. Immunol.* **20**:495–549.
17. Chen, Y., et al. 2006. Anti-IL-23 therapy inhibits multiple inflammatory pathways and ameliorates autoimmune encephalomyelitis. *J. Clin. Invest.* **116**:1317–1326. doi:10.1172/JCI25308.
18. Cua, D.J., et al. 2003. Interleukin-23 rather than interleukin-12 is the critical cytokine for autoimmune inflammation of the brain. *Nature.* **421**:744–748.
19. Murphy, C.A., et al. 2003. Divergent pro- and antiinflammatory roles for IL-23 and IL-12 in joint autoimmune inflammation. *J. Exp. Med.* **198**:1951–1957.
20. Afkarian, M., et al. 2002. T-bet is a STAT1-induced regulator of IL-12R expression in naive CD4+ T cells. *Nat. Immunol.* **3**:549–557.
21. Wang, J., et al. 2006. Transcription factor T-bet regulates inflammatory arthritis through its function in dendritic cells. *J. Clin. Invest.* **116**:414–421. doi:10.1172/JCI26631.
22. Parham, C., et al. 2002. A receptor for the heterodimeric cytokine IL-23 is composed of IL-12Rbeta1 and a novel cytokine receptor subunit, IL-23R. *J. Immunol.* **168**:5699–5708.
23. Kollias, G., and Kontoyiannis, D. 2002. Role of TNF/TNFR in autoimmunity: specific TNF receptor blockade may be advantageous to anti-TNF treatments. *Cytokine Growth Factor Rev.* **13**:315–321.
24. Matsuki, T., Nakae, S., Sudo, K., Horai, R., and Iwakura, Y. 2006. Abnormal T cell activation caused by the imbalance of the IL-1/IL-1R antagonist system is responsible for the development of experimental autoimmune encephalomyelitis. *Int. Immunol.* **18**:399–407.
25. Samoilova, E.B., Horton, J.L., Hilliard, B., Liu, T.S., and Chen, Y. 1998. IL-6-deficient mice are resistant to experimental autoimmune encephalomyelitis: roles of IL-6 in the activation and differentiation of autoreactive T cells. *J. Immunol.* **161**:6480–6486.
26. Veldhoen, M., Hocking, R.J., Atkins, C.J., Locksley, R.M., and Stockinger, B. 2006. TGFbeta in the context of an inflammatory cytokine milieu supports de novo differentiation of IL-17-producing T cells. *Immunity.* **24**:179–189.
27. Shtrichman, R., and Samuel, C.E. 2001. The role of gamma interferon in antimicrobial immunity. *Curr. Opin. Microbiol.* **4**:251–259.
28. Happel, K.I., et al. 2005. Divergent roles of IL-23 and IL-12 in host defense against *Klebsiella pneumoniae*. *J. Exp. Med.* **202**:761–769.
29. Stark, M.A., et al. 2005. Phagocytosis of apoptotic neutrophils regulates granulopoiesis via IL-23 and IL-17. *Immunity.* **22**:285–294.

Role of caveolin-1 in the regulation of the vascular shear stress response

Philippe G. Frank[1,2,3] and Michael P. Lisanti[2,3]

[1]Department of Urology and [2]Departments of Molecular Pharmacology and Medicine and the Albert Einstein Diabetes Research and Training Center (DRTC), Albert Einstein College of Medicine, New York, New York, USA.
[3]Department of Cancer Biology, Kimmel Cancer Center, Thomas Jefferson University, Philadelphia, Pennsylvania, USA.

In blood vessels, endothelia are submitted to constant shear effects and are, under normal conditions, capable of responding to any variation in hemodynamic forces. Caveolae — 50- to 100-nm plasma membrane invaginations present at the surface of terminally differentiated cells and particularly enriched in ECs — are composed of a high sphingolipid and cholesterol content and the protein caveolin-1 (Cav-1). Previous studies have suggested that caveolae and endothelial Cav-1 may regulate the vascular response to altered shear stress. In this issue of the *JCI*, Yu et al. have examined the role of Cav-1/caveolae in the regulation of flow-induced alterations (i.e., mechanotransduction) in vessels from wild-type mice, Cav-1–deficient mice, and Cav-1–deficient mice re-expressing Cav-1 only in ECs. Their data suggest that caveolae/Cav-1 may act as sensors of altered shear stress and that they also organize the signaling response in stimulated ECs (see the related article beginning on page 1284).

Shear stress: an important regulator of endothelial cell function

In the vasculature, blood vessels must respond rapidly to any external stimuli and especially to any physical change related to modifications in shear stress, which is a function of the blood viscosity and the velocity gradient at the arterial wall. In this context, blood vessels need to adapt and adjust their luminal diameters and their physical properties. ECs are the primary targets of these changes, as they are the first cell type exposed to these forces. One of the earliest findings that suggested an important role for ECs in this process was the observation of the ability of ECs to reorient and change shape during exposure to shear stress conditions. When submitted to steady laminar shear stress, ECs reorient in the direction of the flow and become remarkably elongated. These observations were made both in vitro (1) and in vivo (2, 3). These findings have suggested that ECs can respond and adapt to changes in blood flow. In fact, ECs act as sensors to transduce hydrodymanic forces. Not only does the morphology of ECs change, but other important signaling pathways have been shown to be regulated in response to altered shear stress. Several studies have shown that under laminar shear stress, the rate of EC proliferation is reduced compared with static conditions (4, 5). Oscillating and/or disturbed conditions have major effects on the pathology of the vasculature. In this regard, atherosclerotic lesions have been shown to develop primarily at sites of disturbed or altered blood flow, i.e., at bifurcations, branch ostia, and curved regions (6). Under oscillating and/or disturbed conditions, EC proliferation is increased compared with cells submitted to laminar shear stress and may allow ECs to repair injuries (7, 8). Other important regulatory pathways have now been shown to be activated under shear stress conditions (9–11). These pathways include those involved in changes in endothelial apoptotic, migratory, and permeability prop-

Nonstandard abbreviations used: Cav-1, caveolin-1.

Conflict of interest: The authors have declared that no conflict of interest exists.

Citation for this article: *J. Clin. Invest.* **116**:1222–1225 (2006). doi:10.1172/JCI28509.

166

IL-17 Plays an Important Role in the Development of Experimental Autoimmune Encephalomyelitis[1]

Yutaka Komiyama, Susumu Nakae,[2] Taizo Matsuki,[3] Aya Nambu, Harumichi Ishigame, Shigeru Kakuta, Katsuko Sudo,[4] and Yoichiro Iwakura[5]

IL-17 is a proinflammatory cytokine that activates T cells and other immune cells to produce a variety of cytokines, chemokines, and cell adhesion molecules. This cytokine is augmented in the sera and/or tissues of patients with contact dermatitis, asthma, and rheumatoid arthritis. We previously demonstrated that IL-17 is involved in the development of autoimmune arthritis and contact, delayed, and airway hypersensitivity in mice. As the expression of IL-17 is also augmented in multiple sclerosis, we examined the involvement of this cytokine in these diseases using IL-17$^{-/-}$ murine disease models. We found that the development of experimental autoimmune encephalomyelitis (EAE), the rodent model of multiple sclerosis, was significantly suppressed in IL-17$^{-/-}$ mice; these animals exhibited delayed onset, reduced maximum severity scores, ameliorated histological changes, and early recovery. T cell sensitization against myelin oligodendrocyte glycoprotein was reduced in IL-17$^{-/-}$ mice upon sensitization. The major producer of IL-17 upon treatment with myelin digodendrocyte glycopritein was CD4$^+$ T cells rather than CD8$^+$ T cells, and adoptive transfer of IL-17$^{-/-}$ CD4$^+$ T cells inefficiently induced EAE in recipient mice. Notably, IL-17-producing T cells were increased in IFN-$\gamma^{-/-}$ cells, while IFN-γ-producing cells were increased in IL-17$^{-/-}$ cells, suggesting that IL-17 and IFN-γ mutually regulate IFN-γ and IL-17 production. These observations indicate that IL-17 rather than IFN-γ plays a crucial role in the development of EAE. *The Journal of Immunology,* **2006, 177: 566–573.**

The cytokine IL-17 can activate the expression of a variety of proinflammatory cytokines, chemokines, and cell adhesion molecules throughout a wide range of cell types, including macrophages, dendritic cells, T cells, synovial cells, and endothelial cells (1). Augmented expression of this cytokine is observed in patients with various diseases, such as rheumatoid arthritis (RA)[6] (2), systemic lupus erythematosus (3), Behcet's disease (4), allograft rejection (5), nephritic syndrome (6), asthma (7), and multiple sclerosis (MS) (8), suggesting the involvement of IL-17 in the development of these diseases. We have also demonstrated the contribution of IL-17 to the development of allergic and autoimmune diseases in mice, including contact dermatitis, airway inflammation, and arthritis (9–11). IL-17 also plays an important role in the host defense mechanisms protecting against *Klebsiella pneumoniae* infection (12). However, the role of IL-17 has only been elucidated in a few diseases and the role of this cytokine in the pathogenesis of most diseases remains largely unknown.

IL-17 is produced by a variety of cell types. A subset of Th0 and Th1 cell clones, but not Th2 cell clones, that were established from the synovial tissues of RA patients produced IL-17 (13). A number of Th0, Th1, and Th2 clones established from patients with allergic contact dermatitis also produce this cytokine (14). IL-17 is also produced by TNF-α- and/or GM-CSF-producing CD4$^+$ T cells isolated from the synovial fluid of patients with Lyme arthritis, which exhibit neither a Th1 nor a Th2 phenotype (15). Eosinophils from patients with asthma are also reported to produce this cytokine (16). Both lung neutrophils from mice treated with LPS and CD8$^+$ T cells derived from mice infected with *Klebsiella pneumoniae* are producers of IL-17 (17, 18). Thus, the producer cells of IL-17 differ in a manner dependent on the disease.

Experimental autoimmune encephalomyelitis (EAE), a rodent model of human MS, is induced by immunization of mice with encephalitogenic myelin Ags in the presence of adjuvants. EAE pathogenesis is characterized by inflammation of the CNS associated with demyelination and the infiltration of inflammatory cells including neutrophils and encephalitogenic myelin Ag-specific CD4$^+$ T cells. In MS patients, IL-17 mRNA and protein are increased in both brain lesions and mononuclear cells isolated from blood and cerebrospinal fluids (8, 19). IL-17 is also increased in lymphocytes derived from mice with EAE (20). Although these observations suggest that IL-17 may contribute to the development of MS and EAE, the precise role of this cytokine in the pathogenesis of these diseases is still poorly understood.

In this report, we have investigated the role of IL-17 in the development of the EAE using IL-17$^{-/-}$ mice. We demonstrated that the development of EAE was markedly suppressed in IL-17$^{-/-}$ mice. We also determined that IL-17 was important for the optimal activation of myelin oligodendrocyte glycoprotein

Center for Experimental Medicine, Institute of Medical Science, University of Tokyo, Tokyo, Japan

Received for publication August 30, 2005. Accepted for publication April 7, 2006.

The costs of publication of this article were defrayed in part by the payment of page charges. This article must therefore be hereby marked *advertisement* in accordance with 18 U.S.C. Section 1734 solely to indicate this fact.

[1] This work was supported by grants from the Ministry of Education, Culture, Sports, and Science of Japan, and the Ministry of Health and Welfare of Japan.

[2] Current address: Department of Pathology, Stanford University School of Medicine, 269 Campus Drive, Center for Clinical Sciences Research 3255, Stanford, CA 94305-5176.

[3] Current address: ERATO Yanagisawa Orphan Receptor Project, Japan Science and Technology Agency, Koto-Ku, Japan.

[4] Current address: Animal Research Center, Tokyo Medical University, Sinjyuku-ku, Tokyo 160-8402, Japan.

[5] Address correspondence and reprint requests to Dr. Yoichiro Iwakura, Center for Experimental Medicine, Institute of Medical Science, University of Tokyo, 4-6-1 Shirokanedai, Minato-ku, Tokyo 108-8639, Japan. E-mail address: iwakura@ims.u-tokyo.ac.jp

[6] Abbreviations used in this paper: RA, rheumatoid arthritis; MS, multiple sclerosis; EAE, experimental autoimmune encephalomyelitis; MOG, myelin oligodendrocyte glycoprotein; PTx, pertussis toxin; LN, lymph node; rm, recombinant human; GVHR, graft-vs-host reaction; CIA, collagen-induced arthritis; IDDM, insulin-dependent diabetes mellitus.

Copyright © 2006 by The American Association of Immunologists, Inc.

0022-1767/06/$02.00

(MOG)-specific T cells. In this model, $CD4^+$ T cells were the major producers of IL-17 in this system.

Materials and Methods

Mice

IL-$17^{-/-}$ mice (9), generated as described previously, were backcrossed to the C57BL/6J strain (six or nine generations). C57BL/6J and IFN-$\gamma^{-/-}$ mice, both on the C57BL/6J background were purchased from Japan SLC and from The Jackson Laboratory, respectively. Mice were kept under pathogen-free conditions in an environmentally controlled clean room at the Center for Experimental Medicine, Institute of Medical Science, University of Tokyo. All experiments were conducted according to the institutional ethical guidelines for animal experimentation and the safety guidelines for genetic manipulation experiments.

Induction of EAE

Active EAE. The MOG_{35-55} peptide (MEVGWYRSPFSRVVHLYRNGK) was synthesized and purified by HPLC at our institute (Dr. S. Imajoh-Ohmi, Division of Molecular Biology, Institute of Medical Science, University of Tokyo). Mice (8–13 wk of age) were immunized s.c. in one flank on day 0 and in the other on day 7 with 300 μg of MOG_{35-55} peptide emulsified in CFA (1:1), which consisted of IFA with 5 mg/ml *Mycobacterium tuberculosis* H37RA (Difco Laboratories). Pertussis toxin (PTx; Alexis) (200 ng) was injected i.v. on days 0 and 2. Following the first immunization, the severity of EAE was monitored and graded on a scale of 0–5: 0, no disease; 1, limp tail; 2, hind limb weakness; 3, hind limb paralysis; 4, hind and fore limb paralysis; 5, moribundity and death.

Passive EAE. Mice were immunized s.c. with MOG/CFA. Ten days after the immunization, the spleen and inguinal and axillary lymph nodes (LNs) were collected and a single-cell suspension was prepared. Pooled lymphocytes (4×10^6 cells/ml) were cultured in the presence of 50 μg/ml MOG_{35-55} peptide in RPMI 1640 medium containing 50 μM 2-ME, 50 μg/ml streptomycin, 50 μg/ml penicillin, and 10% heat-inactivated FBS (Sigma-Aldrich) for 4 days. After harvesting, $CD4^+$ T cells were purified by positive selection using an AutoMACS system (Miltenyi Biotec). Isolated $CD4^+$ T cells (4×10^6) were then transferred i.v. into naive C57BL/6J mice.

Histology

On day 42 after the first immunization with MOG/CFA and PTx, spines were harvested and fixed with neutral 10% formalin. Spinal cords were then extracted and embedded in paraffin. Sections (5 μm) were stained with H&E.

MOG-specific LN cell proliferation assay

Mice were immunized s.c. with MOG/CFA. Ten days after immunization, the inguinal and axillary LNs were collected and a single-cell suspension was prepared. LN cells ($1-4 \times 10^5$ cells/well) were cultured for 72 h in the absence or presence of various concentrations of MOG_{35-55} peptide as described above. Isolated cells were then pulsed for 6 h with [^{3}H]thymidine (0.25 μCi/ml; Amersham Biosciences), and harvested using a Micro 96 cell harvester (Skatron). Levels of radioactivity were measured using a Micro β system (Pharmacia Biotech).

Measurement of cytokine levels by ELISA

To detect IFN-γ and IL-4 in culture supernatants, we used mouse IFN-γ OptEIA kit (BD Pharmingen) and IL-4 ELISA kit (Endogen). Detection of IL-17 by ELISA was performed as described previously (9).

Flow cytometry

To examine LN cell population, inguinal and axillary LN cells were harvested 10 days after immunization with MOG/CFA. After incubation of cells on ice with anti-mouse CD16/CD32 mAb (2.4G2) in a staining buffer (Hank's buffer containing 2% FCS and 0.1% sodium azide) on ice for 15 min, cells were incubated on ice for 45 min with either FITC-anti-mouse CD45RB (C363.16A) or FITC anti-mouse CD62L (MEL-14) in the presence of PE anti-mouse CD44 (Pgp-1) and allophycocyanin anti-mouse CD4 (RM4-5). 7-Aminoactinomycin D (Sigma-Aldrich)-negative, $CD4^+$ cells were examined by a FACSCalibur (BD Biosciences) using CellQuest software (BD Biosciences). To detect IL-17 production in lymphocytes (T cells and B cells), LN cells were harvested 10 days after immunization with MOG/CFA. Isolated cells were cultured in the presence or absence of 50 μg/ml MOG_{35-55} peptide for 72 h as described above. To examine IL-17 production by Gr-1^+ neutrophils, we prepared a single-cell suspension from the spleens of EAE-affected wild-type mice (day 42). LN cells (72 h after cultivation) and spleen cells were stimulated for 6 h with 20 ng/ml PMA (Sigma-Aldrich), 1 μM ionomycin (Sigma-Aldrich), and 2 μM monensin (Sigma-Aldrich) for 6 h. After harvesting, cells were incubated on ice with anti-mouse CD16/CD32 mAb (2.4G2) in a staining buffer on ice for 15 min. Cell samples were then incubated on ice for 45 min with either FITC-anti-mouse B220 (RA3-6B2), FITC anti-mouse Gr-1 (RB6-8C5), or FITC anti-mouse CD3ε (145-2C11), allophycocyanin anti-mouse CD4 (RM4-5 or GK1.5), or allophycocyanin anti-mouse CD8α (53-6.7) Abs. After washing, the cells were fixed in a fixation buffer (2% paraformaldehyde in PBS) at room temperature for 10 min. Samples were then permeabilized with permeabilization buffer (staining buffer containing 0.1% saponin) and incubated for 30 min with PE-conjugated anti-mouse IL-17 mAb (TC11-18H10) or isotype-matched control rat IgG1 (R3-34) at 4°C. The cells were analyzed on a FACSCalibur flow cytometer as described above. All mAbs were purchased from BD Pharmingen.

$CD4^+$ T cell cultures

$CD4^+$ T cells (< 95%) from wild-type mouse spleen were purified by MACS system as described elsewhere (9), then stimulated with 1.0 μg/ml plate-coated anti-CD3 mAb (145-2C11; BD Pharmingen) in the presence or absence of various concentration of recombinant mouse IFN-γ

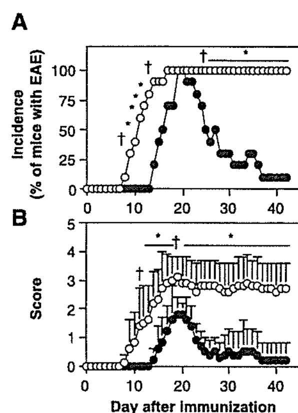

FIGURE 1. Development of EAE was reduced in IL-$17^{-/-}$ mice. EAE was induced in mice by immunization with MOG/CFA coinjected with PTx. *A*, Incidence of EAE. *B*, Clinical scores of diseased mice. ○, Wild-type mice (n = 10); ●, IL-$17^{-/-}$ mice (n = 10). Data are the averages ± SD for each group. †, $p < 0.05$ and *, $p < 0.001$ vs IL-$17^{-/-}$ mice by Mann-Whitney's U test (*A*) and by χ^2 test (*B*), respectively.

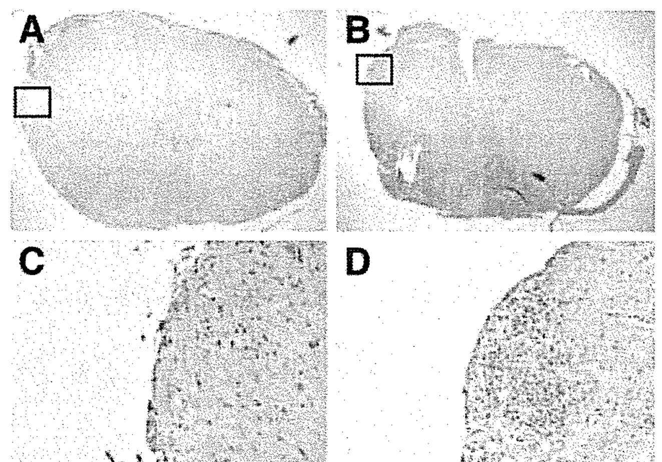

FIGURE 2. Local inflammation of the CNS was suppressed in IL-$17^{-/-}$ mice during EAE. On day 42 after MOG/CFA and PTx immunization, spinal cords were removed. The tissue sections were stained with H&E. The sections at the lumbar level are shown. *A* and *C*, IL-$17^{-/-}$ mice. *B* and *D*, Wild-type mice. *A* and *B*, ×40. *C* and *D*, ×200.

(rmIFN-γ; PeproTech), rmIL-12 (R&D Systems), rmIL-17 (R&D Systems), and rmIL-23 (R&D Systems) for 48 h. Then, culture supernatants were collected and IFN-γ or IL-17 levels in the supernatants were determined by ELISA as described above.

Measurement of MOG-specific serum Ab levels by ELISA

A 96-well flat-bottom plate (Falcon 3912 Micro test III Flexible Assay Plates; BD Biosciences) was coated with 10 μg/ml MOG_{35-55} peptides at 4°C overnight. After washing the wells with 0.05% Tween 20 in PBS, the wells were blocked with PBS containing 1% skim milk, 5 mM EDTA, 0.02% NaN3 for 1 h at room temperature. After washing, diluted serum samples were added and incubated for 2 h at room temperature. Then, after washing the wells, alkaline phosphatase-conjugated goat anti-mouse Igs (IgG, IgG1, IgG2a, IgG2b, IgG3, IgM; Zymed Laboratories) were added and incubated for 1 h at room temperature. Alkaline phosphatase activity was measured using Substrate Phosphatase SIGMA104 (Sigma-Aldrich). The anti-MOG Ab titer was shown as OD_{415} values.

Statistics

The Student *t* test, the Mann-Whitney's *U* test, or the χ^2 test was used for the statistical evaluation of the results.

Results

Development EAE was suppressed in IL-17$^{-/-}$ mice

To investigate the role of IL-17 in the pathogenesis of EAE, we examined the effect of IL-17-deficiency on the development of EAE using IL-17$^{-/-}$ mice. To induce EAE, mice were treated with MOG_{35-55} peptide emulsified in CFA and injected with PTx. The initial signs of EAE were observed 10 days after the first immunization of wild-type mice (Fig. 1). In contrast, the onset of EAE was significantly delayed in IL-17$^{-/-}$ mice until day 15 (Fig. 1). Twenty days after the first immunization, however, IL-17$^{-/-}$ mice exhibited a similar incidence of EAE as that seen in wild-type mice (Fig. 1*A*), although the severity of disease in IL-17$^{-/-}$ mice was milder than that in wild-type mice (Fig. 1*B*). After day 20 from the immunization, the severe signs of disease continued in wild-type mice, while early amelioration was observed in IL-17$^{-/-}$ mice (Fig. 1*A*). Consistent with these observations, a massive infiltration of mononuclear cells was observed within the spinal cords of wild-type mice 42 days after the first immunization (Fig. 2, *B* and *D*). In contrast, the cellular infiltration was significantly reduced in IL-17$^{-/-}$ mice (Fig. 2, *A* and *C*).

PTx is widely used to enhance the development of T cell-mediated organ-specific autoimmune diseases, including EAE. TNF-α$^{-/-}$ mice develop EAE normally when high doses of PTx are injected, while in the presence of low doses of PTx, mutant mice exhibit significantly reduced development of EAE symptoms (21). Thus, PTx may sometimes mask or compensate for the pathological functions of some proinflammatory mediators, such as TNF-α, in the pathogenesis of EAE. Therefore, to more clearly observe the effect of IL-17 deficiency, we next induced EAE in IL-17$^{-/-}$ mice in the absence of PTx treatment. Under these conditions, disease onset in IL-17$^{-/-}$ mice delayed compared with wild-type mice similarly to that seen in the presence of PTx (Fig. 3). Interestingly, in the absence of PTx, the disease also gradually ameliorated in wild-type mice after 22 days of induction, as seen for IL-17$^{-/-}$ mice, although the maximal severity score of the wild-type mice remained significantly higher (Fig. 3). These results demonstrate that IL-17 contributes to the development of EAE.

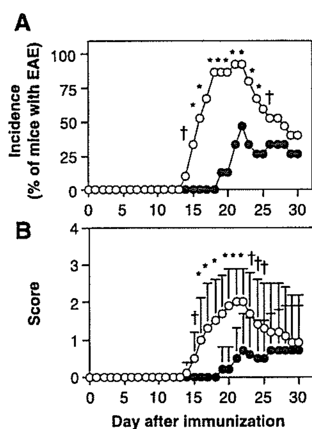

FIGURE 3. Development of EAE was reduced in IL-17$^{-/-}$ mice. Mice were induced EAE by immunization with MOG/CFA, but without PTx. *A*, Incidence of EAE. *B*, Clinical score of diseased mice. ○, Wild-type mice ($n = 15$), and ●, IL-17$^{-/-}$ mice ($n = 15$). Data are shown as an average + SD in each group. †, $p < 0.05$ and *, $p < 0.001$ vs IL-17$^{-/-}$ mice by Mann-Whitney's *U* test (*A*) and by χ^2 test (*B*).

MOG- specific T cell sensitization was impaired in IL-17$^{-/-}$ mice

We previously showed that IL-17 plays an important role in Ag-specific T cell activation during the development of multiple allergic and autoimmune diseases (9–11). To compare our previous

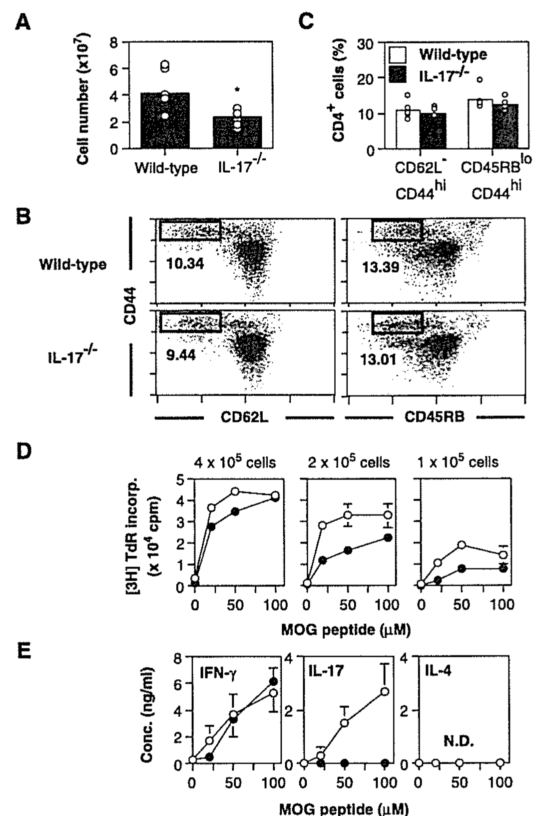

FIGURE 4. MOG-specific lymphocyte activation was impaired in IL-17$^{-/-}$ mice. Mice were immunized once with MOG/CFA in the absence of PTx, and 10 days after immunization, the inguinal and axillary LNs were collected and pooled. *A*, Total LN cell number. *B* and *C*, Percentage of CD62L$^-$CD44^{high} or CD45RB^{low}CD44^{high} CD4$^+$ T cells in LNs. In *A* and *C*, each circle represents a value from an individual mouse, and the column represents the average for each group. Representative FACS results are shown in *B*. *, $p < 0.05$ and vs the corresponding values for wild-type mice. *D*, Isolated LN cells were cultured in the absence or presence of MOG peptide for 72 h, and MOG-specific LN cell proliferation as measured by [^{3}H]thymidine incorporation (*D*) and IFN-γ, IL-17, and IL-4 levels in the culture supernatants (2 × 10^5 cells) (*E*) are shown. ○, Wild-type mice, and ●, IL-17$^{-/-}$ mice. Averages ± SD of triplicate wells are shown. All results are representative at least in three experiments. *D*, Data are averages ± SD from three independent experiments. N.D., Not detected.

results to the models in the current study, we next assessed the role of IL-17 in the activation of MOG-specific T cells during the development of EAE. Ten days after immunization with MOG/CFA alone (without PTx), hypertrophy of inguinal and axillary lymph nodes was observed. Although the total number of pooled inguinal and axillary LN cells was significantly decreased in IL-$17^{-/-}$ mice in comparison with wild-type mice (Fig. 4*A*), the content of memory $CD4^+$ T cells ($CD62L^-CD44^{high}$ or $CD45RB^{low}CD44^{high}$) was comparable (Fig. 4, *B* and *C*). Then, the draining LN cells were cultured in the presence or absence of MOG peptide. When a large excess of LN cells (4×10^5 cells) was present in a well, the observed MOG-specific LN cell proliferative responses in IL-$17^{-/-}$ mice were similar to those seen in wild-type LN cells (Fig. 4*D*). In the presence of an optimal number of LN cells (2×10^5 and 1×10^5 cells), the proliferative responses of cells derived from IL-$17^{-/-}$ mice were markedly decreased compared with those in wild-type mice despite similar number of memory T cells was contained in wild-type and IL-$17^{-/-}$ mouse culture (Fig. 4*D*). IL-17 was detected in the supernatants of wild-type LN cell cultures (2×10^5 cells), and its levels increased in a manner dependent on the dose of MOG peptide. IL-17 was undetectable in IL-$17^{-/-}$ LN cell cultures (2×10^5 cells) (Fig. 4*D*). The MOG-specific proliferative responses of LN T cells were reduced in IL-$17^{-/-}$ mice (Fig. 4D). Nevertheless, IFN-γ production in the LN cell culture supernatants was similar in wild-type and IL-$17^{-/-}$ mice (Fig. 4*E*). IL-4 levels in the LN cell culture supernatants from both wild-type and IL-$17^{-/-}$ mice were below the limit of detection (Fig. 4*E*). These results suggest that the delayed onset of the EAE response in IL-$17^{-/-}$ mice is caused by insufficient T cell sensitization against the MOG peptide.

$CD4^+$ T cells produced IL-17 in LN cells during EAE

Different subsets of $CD4^+$ Th cells and eosinophils are known to produce IL-17 in patients with dermatitis, RA, Lyme arthritis, and asthma (13–16). Neutrophils and $CD8^+$ T cells can also produce IL-17 during certain infectious diseases in mice (17, 18). These observations suggest that the IL-17 producer cells may differ from those known to produce this cytokine in other diseases. Thus, we next analyzed the IL-17 producer cells in the LNs of wild-type mice following MOG immunization. Ten days after immunization, inguinal and axillary LNs were collected and LN cells were cultured in the presence of MOG peptide for 72 h. After MOG stimulation, IL-17 production was detected in $CD3^+$ T cells, but not in granulocytes or B cells (Fig. 5*A*). Within the T cell population, IL-17 was predominantly produced in $CD4^+$ T cells, but at low levels in $CD8^+$ T cells (Fig. 5*B*). Thus, $CD4^+$ T cells, rather than $CD8^+$ T cells, were the major producer of IL-17 within LNs during the development of EAE.

The efficiency of EAE induction of IL-$17^{-/-}$ CD4 T cells was low in comparison with wild-type T cells

To examine the effect of IL-17 deficiency on T cell sensitization against the MOG peptide, we adoptively transferred $CD4^+$ T cells into recipient mice of the same genetic background. Lymphocytes from MOG/CFA-immunized wild-type or IL-$17^{-/-}$ mice were stimulated with MOG peptide for 4 days in vitro, and $CD4^+$ T cells were then purified and transferred into naive wild-type mice. The development of EAE in mice that received IL-$17^{-/-}$ $CD4^+$ T cells was markedly reduced in comparison to those animals receiving wild-type $CD4^+$ T cells (Fig. 6). These observations indicate that MOG-specific T cells from IL-$17^{-/-}$ mice cannot efficiently induce EAE in recipient mice.

IL-17 production was enhanced in IFN-$\gamma^{-/-}$ mice

MS and EAE are typically classified as Th1 cell-mediated autoimmune diseases. It has been shown, however, that the development of EAE is exacerbated in IFN-$\gamma^{-/-}$ and/or IFN-$\gamma R^{-/-}$ mice (22–25), indicating that IFN-γ serves a protective role in the disease pathogenesis. Therefore, we next examined whether IFN-γ-deficiency influences IL-17 production by $CD4^+$ T cells during EAE development. Consistent with previous reports, the LN (inguinal and axillary) cell number of IFN-$\gamma^{-/-}$ mice was significantly increased compared with that of wild-type mice 10 days after MOG/CFA immunization (Fig. 7*A*). When LN cells from MOG-immunized mice were cultured in the presence of MOG peptides, proliferating cells were predominantly observed in a region indicated as "R2", while nonproliferating cells were observed in a region indicated as "R1" (Fig. 7*B*), as determined by CFSE labeling (data not shown). Thus, to detect MOG-reactive, IL-17-producing T cells in LN cells, cells were selectively gated to the R2 region. The percentage of IL-17-producing $CD4^+$ T cells in the draining LN cells of IFN-$\gamma^{-/-}$ mice was greatly increased in comparison to that in wild-type mouse T cells, irrespective of MOG restimulation (Fig. 7, *C* and *D*). A large proportion of $CD8^+$ T cells, as well as $CD4^+$ T cells from IFN-$\gamma^{-/-}$ mice immunized with MOG/CFA, produced IL-17, although only a small proportion of $CD8^+$ cells from wild-type mice produced IL-17 (Fig. 7, *C* and *D*).

Next, we assessed the effect of IL-17 on IFN-γ production during MOG immunization. As shown in Fig. 4, *D* and *E*, although MOG-specific T cell proliferation was impaired in IL-$17^{-/-}$ mice, IFN-γ levels in culture supernatants were normally observed. These observations suggested that the IFN-γ-producing cell population is increased in IL-$17^{-/-}$ mice. In support of this, the percentage of IFN-γ-producing $CD4^+$ T cells in the draining LN cells

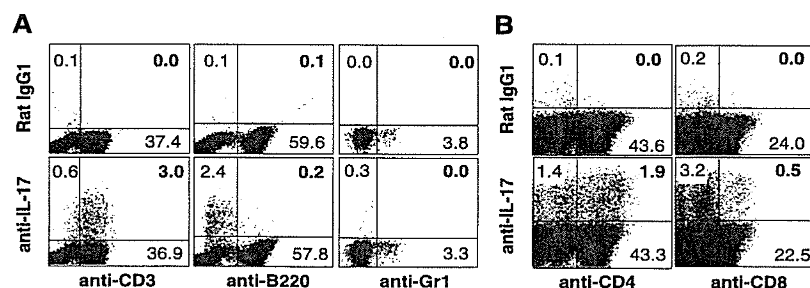

FIGURE 5. IL-17 was primarily produced by $CD4^+$ LN T cells during the development of EAE. To detect IL-17-producing cells in the lymphocyte or granulocyte populations, LN cells from mice immunized with MOG/CFA were cultured in the presence of 50 μg/ml MOG peptide for 72 h, followed by stimulation with PMA + ionomycin in the presence of monensin; then IL-17-producing cells were detected by FACS. Gr-1^+ cells were stained using spleen cells from mice with EAE. *A*, The IL-17^+ populations in $CD3^+$ or $B220^+$ cell populations within the LN cells, or the Gr-1^+ cells of the spleen. *B*, IL-17 production by $CD3^+CD4^+$ or $CD3^+CD8^+$ T cells.

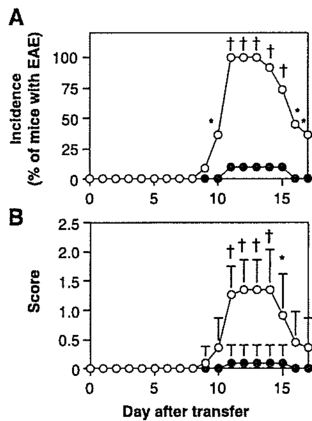

FIGURE 6. $CD4^+$ T cells were responsible for the induction of EAE. Mice were immunized once with MOG/CFA alone. At 10 days postimmunization, the spleen and the inguinal and axillary LNs were collected and pooled. The pooled cells were cultured in the presence of MOG peptide for 72 h, and then $CD4^+$ T cells were purified and transferred into naive, wild-type mice. *A*, The incidence of EAE. *B*, The clinical scores of the diseased mice. ○, Mice that received wild-type $CD4^+$ T cells ($n = 11$), and, ●, mice that received IL-$17^{-/-}$ $CD4^+$ T cells ($n = 10$). In *B*, data are shown as the averages ± SD for each group. †, $p < 0.05$ and *, $p < 0.001$ vs IL-$17^{-/-}$ mice by the Mann-Whitney's *U* test (*A*) and by the χ^2 test (*B*), respectively.

of IL-$17^{-/-}$ mice was significantly increased compared with that in wild-type mice after MOG stimulation (Fig. 8). Similar results were also obtained in $CD8^+$ T cells (Fig. 8). Thus, these data suggest that IL-17 production is regulated by IFN-γ while IFN-γ is regulated by IL-17.

Then, we examined whether IL-17 and IFN-γ can directly regulate IFN-γ and IL-17 production, respectively. When purified splenic $CD4^+$ T cells were stimulated with plate-coated anti-CD3 mAb in the presence of various concentration of IL-12, IFN-γ production was enhanced in a dose-dependent manner (Fig. 9*A*). However, IL-17 did not influence IFN-γ production by $CD4^+$ T cells in the absence or presence of IL-12 (Fig. 9, *B* and *C*). IL-23 could promote IL-17 production dose dependently (Fig. 9*D*), while IFN-γ did not show any effects on IL-17 production irrespective of the presence of IL-23 (Fig. 9, *E* and *F*). These observations indicate that IFN-γ or IL-17 cannot directly modulate IL-17 or IFN-γ production.

Increased MOG-specific Ab production in IL-$17^{-/-}$ mice during EAE

To elucidate the role of IL-17 in MOG-specific Ab production, we measured the level of anti-MOG-specific serum Abs in wild-type and IL-$17^{-/-}$ mice during EAE. Before immunization with MOG peptides, the level of MOG-specific IgG was very low in both wild-type and IL-$17^{-/-}$ mice (Fig. 10*A*). On day 20 after MOG/CFA immunization with PTx injection as shown in Fig. 1, the level of MOG-specific IgG in IL-$17^{-/-}$ mice was slightly higher than that in wild-type mice (Fig. 10*A*). In chronic inflammatory phases during EAE induced by MOG/CFA with PTx, the levels of MOG-specific IgG and IgG1 in IL-$17^{-/-}$ mice were profoundly increased compared with these in wild-type mice, although these IL-$17^{-/-}$ mice did not show any sign of EAE (Fig. 10). Similarly, the levels of MOG-specific IgG2a and IgG2b were also slightly, but not significantly, increased in IL-$17^{-/-}$ mice, while those of MOG-specific IgG3 and IgM were not different between wild-type and IL-$17^{-/-}$ mice (Fig. 10*B*). These results indicated that IL-17 has an influence upon MOG-specific Ab production by B cells.

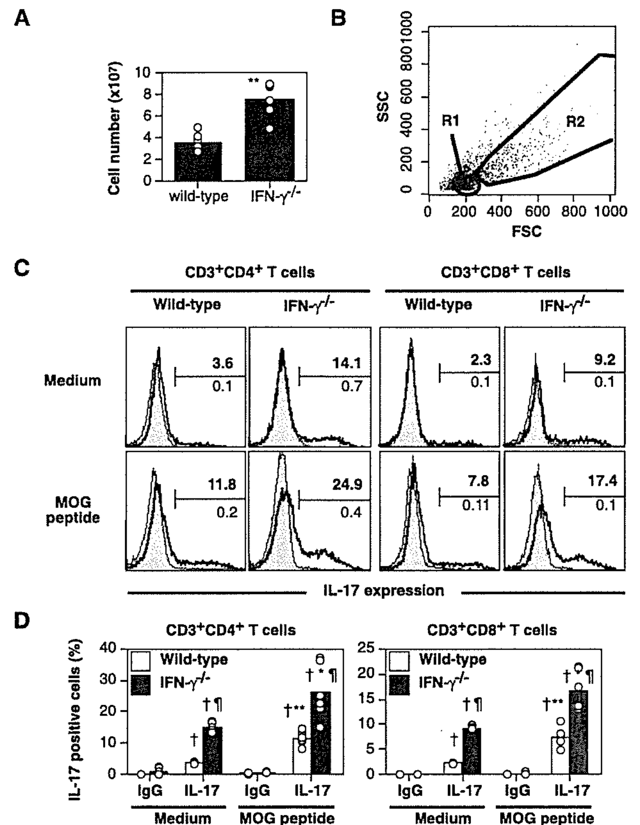

FIGURE 7. The proportion of IL-17-producing $CD4^+$ and $CD8^+$ T cells was increased in IFN-$\gamma^{-/-}$ mice after MOG immunization. LN cells from mice immunized with MOG/CFA were cultured for 72 h in the presence or absence of 50 μg/ml MOG peptide. IL-17-producing cells were then analyzed by FACS, and the percentage of IL-$17^+CD3^+CD4^+$ T cells is shown. *A*, Total LN cell number from inguinal and axillary LNs from wild-type ($n = 6$) and IFN-$\gamma^{-/-}$ ($n = 6$) mice. **, $p < 0.01$ vs wild-type mice. *B*, Gating in FACS analysis, R2 rather than R1 contained MOG-specific proliferating cells using CFSE labeling. *C*, Staining of intracellular IL-17 in $CD3^+CD4^+$ or $CD3^+CD8^+$ T cells stimulated with or without MOG peptides. Shaded areas, staining with isotype-matched control Ab; bold lines, anti-mouse IL-17 staining. The percentage of IL-17-positive cells (upper bold figures) and percentage of cells which were stained with an isotype-matched control IgG (lower figures) are shown. *D*, Each circle represents a value from an individual mouse, and the column represents the average for each group in *C*. □, Wild-type mice ($n = 6$). ■, IFN-$\gamma^{-/-}$ mice ($n = 6$). IgG, isotype-matched control IgG staining. IL-17, anti-mouse IL-17 staining. †, $p < 0.05$ vs the corresponding values for control IgG staining. *, $p < 0.05$ and **, $p < 0.01$ vs the corresponding values for the cultures in the absence of MOG peptide (medium alone). ¶, $p < 0.05$ vs the corresponding values of wild-type mice. All p values were determined by the Student's *t* test.

However, our findings suggest that no correlation exists between the susceptibility and severity of EAE and the levels of anti-MOG Abs in IL-$17^{-/-}$ mice.

Discussion

In this study, we have demonstrated using IL-$17^{-/-}$ mice that IL-17 plays an important role in the development of EAE induced by MOG/CFA. We found that, upon immunization with MOG/CFA, T cell sensitization was defective in IL-$17^{-/-}$ mice, and $CD4^+$ T cells from IL-$17^{-/-}$ mice did not induce EAE efficiently compared with wild-type T cells. These observations suggest that IL-17 plays an important role in the activation of encephalitogenic T cells during the sensitization phase of EAE. In contrast, it was recently reported that IL-17-producing $CD4^+$ T cells enhance the

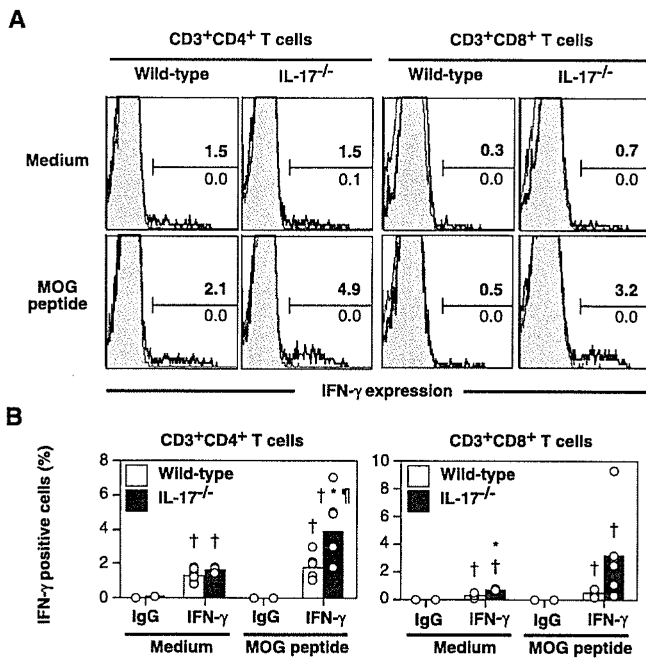

FIGURE 8. The proportion of IFN-γ-producing $CD4^+$ and $CD8^+$ T cells was increased in IL-$17^{-/-}$ mice after MOG immunization. LN cells from mice immunized with MOG/CFA were cultured for 72 h in the presence or absence of 50 μg/ml MOG peptide. IFN-γ-producing cells were then analyzed by FACS, and the percentage of IFN-$\gamma^+CD3^+CD4^+$ or $CD3^+CD8^+$ T cells is shown. *A*, Staining of intracellular IFN-γ in $CD3^+CD4^+$ or $CD3^+CD8^+$ T cells stimulated with or without MOG peptides. Shaded areas, staining with isotype-matched control Ab; bold lines, anti-mouse IFN-γ staining. The percentage of IFN-γ-positive cells (upper bold figures) and percentage of cells which were stained with an isotype-matched control IgG (lower figures) are shown. *B*, Each circle represents a value from an individual mouse, and the column represents the average for each group in *A*. □, Wild-type mice ($n = 6$). ■, IL-$17^{-/-}$ mice ($n = 6$). IgG, isotype-matched control IgG staining. IFN-γ, anti-mouse IFN-γ staining. †, $p < 0.05$ vs the corresponding values for control IgG staining. *, $p < 0.05$ vs the corresponding values for the cultures in the absence of MOG peptide (medium alone). ¶, $p < 0.05$ vs the corresponding values of wild-type mice. All p values were determined by the Student t test.

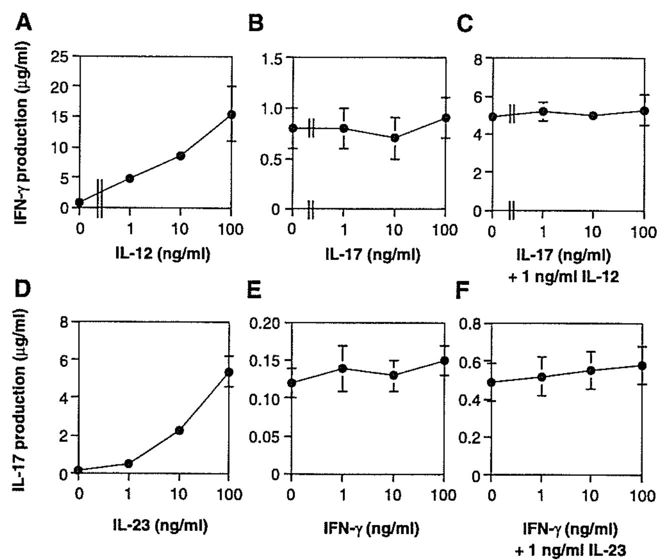

FIGURE 9. Exogenous IFN-γ and IL-17 did not directly affect IL-17 and IFN-γ production by $CD4^+$ T cells. $CD4^+$ T cells from spleen of wild-type mice were stimulated with plate-coated anti-CD3 mAb in the presence or absence of rmIL-17 or rmIFN-γ with or without rmIL-12 or rmIL-23 for 48 h. Then, IFN-γ or IL-17 levels in culture supernatants were determined by ELISA. IFN-γ levels in culture supernatants from $CD4^+$ T cells: stimulated with anti-CD3 mAb plus the indicated amount of rmIL-12 (*A*), rmIL-17 (*B*), and 1 ng/ml rmIL-12 + indicated amount of rmIL-17 (*C*). IL-17 levels in culture supernatants from $CD4^+$ T cells: stimulated with anti-CD3 mAb plus rmIL-23 (*D*), rmIFN-γ (*E*), or 1 ng/ml rmIL-23 + indicated amount of rmIFN-γ (*F*). Data showed the average ± SD from three mice, and a representative result from two independent experiments.

disease severity of EAE and that treatment with anti-IL-17 neutralizing Abs during the elicitation phase suppressed disease development (26). These observations strongly suggest that IL-17 is involved in the pathogenesis of EAE during both the sensitization and elicitation phases.

As Th1 cells, which are the major producers of IFN-γ, infiltrate the inflamed lesions of EAE or collagen-induced arthritis (CIA) (27, 28), it was suspected that IFN-γ may have a pathological role in the development of these autoimmune diseases. However, administration of neutralizing Abs for IFN-γ leads to exacerbation of these diseases (29). The development of CIA is enhanced in IFN-$\gamma^{-/-}$ mice and that of EAE is also exacerbated in both IFN-$\gamma^{-/-}$ and IFN-$\gamma R^{-/-}$ mice compared with wild-type mice (22–25). Thus, IFN-γ may have a protective role in these diseases, rather than a pathogenic role. Consistent with this notion, the development of EAE is also exacerbated in mice deficient for IL-12 p35, a subunit of IL-12 that is required for the differentiation of IFN-γ-producing Th1 cells (30, 31). In a similar manner, the severity of EAE was exaggerated in mice deficient in IL-12Rβ2. Interestingly, we found that the IL-17-producing T cell population was increased in IFN-$\gamma^{-/-}$ mice in comparison to that seen in wild-type mice upon immunized with MOG/CFA (Fig. 7). Similar observations were also currently reported by other groups (32, 33). IL-17 production was also augmented in the splenocytes of IL-12R$\beta2^{-/-}$ mice (20). These observations suggest that IFN-γ plays a beneficial role during the development of EAE by regulating IL-17 production. However, we demonstrated that IFN-γ did not directly influence IL-17 production by $CD4^+$ T cells (Fig. 9, *E* and *F*), suggesting that the suppressive effect of IFN-γ on IL-17 production may be due to the suppression of the development of IL-17-producing cells. In this context, it was recently reported that IL-17-producing cells are induced by IL-23, while IL-12/IFN-γ suppresses the production of IL-17 (34).

We also found that IFN-γ-producing $CD4^+$ and $CD8^+$ T cells were markedly increased in IL-$17^{-/-}$ mice stimulated with MOG peptides, although IL-17 did not show any direct effect on IFN-γ production by $CD4^+$ T cells (Fig. 9, *B* and *C*) (Fig. 8). These observations suggest that IL-17 negatively regulates the development of IFN-γ-producing Th1 cells. Thus, IL-17 and IFN-γ may mutually regulate the development of these cytokine producer cells during immune responses.

We demonstrated that $CD4^+$ T cells are the predominant producers of IL-17 in LN cells after immunization with MOG/CFA. It has been reported that, in Lyme arthritis, IL-17 is primarily produced by a specific subpopulation of $CD4^+$ T cells that are neither Th1 nor Th2 and that produce TNF-α and/or GM-CSF simultaneously. As IL-17 is produced by multiple cell types, including $CD8^+$ T cells, γδ T cells, neutrophils, and eosinophils under different conditions (13–18, 35), the production of IL-17 is not limited to a specific T cell population. Instead, the producer cells in a particular disease appear to be defined by a specific cell population. The mechanism by which these IL-17 producer cells are controlled in different diseases, however, remains to be elucidated.

In MS patients, elevation of anti-MOG Ab levels is detectable in cerebrospinal fluid (36, 37). In association with the elevation of

72

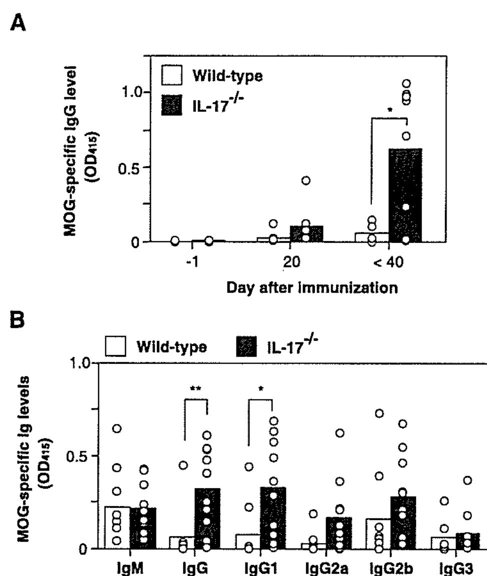

FIGURE 10. Enhanced MOG-specific Ig production in IL-$17^{-/-}$ mice during EAE. MOG-specific Ig levels in sera from wild-type and IL-$17^{-/-}$ mice that developed EAE were determined by ELISA. *A*, As performed in Fig. 1*A*, sera were collected from mice before (−1 day) and after MOG immunization (20 and <40 days). Then, MOG-specific IgG levels in sera were measured. *B*, On day 42 after MOG immunization, MOG-specific IgM, IgG, IgG1, IgG2a, IgG2b, and IgG3 levels in sera were determined. Each circle represents the value from an individual mouse, and a column shows the average of each group. □, Wild-type mice (n = 7). ■, IL-$17^{-/-}$ mice (n = 10). *, $p < 0.05$ and **, $p < 0.01$ for the comparisons shown in brackets by Student's t test.

anti-MOG Abs following immunization with MOG peptides (38), severe demyelination occurred in the Lewis rat, suggesting that the generation of myelin-specific Abs may be involved in the development of EAE. However, we observed that anti-MOG Ab levels were increased in IL-$17^{-/-}$ mice in comparison with the levels seen in wild-type mice after immunization with MOG, while the development of EAE was markedly suppressed in IL-$17^{-/-}$ mice (Fig. 10). Thus, in IL-$17^{-/-}$ mice, there is no apparent correlation between the severity of EAE and the elevation of anti-MOG Abs in IL-$17^{-/-}$ mice, suggesting that anti-MOG Abs are not directly involved in the development of this disease. In fact, the serum MOG-specific Ab levels in mice that developed EAE after the transfer of MOG-specific $CD4^+$ T cells were below the limits of detection (data not shown). In support of this notion, B cell-deficient mice develop EAE normally (39–41). It was reported, however, that Abs are involved in the remyelination of the lesions in the CNS during disease resolution (42). We did not expect that Ab levels specific for MOG would be enhanced in IL-$17^{-/-}$ mice, because Ab production was suppressed in IL-$17^{-/-}$ mice during CIA and contact, delayed-type, and airway hypersensitivity (9–11). We do not currently understand the reasoning for this. The molecular nature of the Ags involved in the autoimmune disorders, however, appears to affect the sensitivity of the disease to IL-17. Additional experiments will be necessary to elucidate the mechanism.

We previously reported that IL-17 is not essential for the induction of graft-vs-host reaction (GVHR) (9), in which $CD8^+$ T cell-derived FasL and perforin play important roles (43, 44). Likewise, IL-17-deficiency did not affect the incidence of hyperglycemia in NOD mice (T. Matsuki, S. Nakae, and Y. Iwakura, unpublished observations), although IL-17 mRNA expression is increased in NOD mice upon development of insulin-dependent diabetes mellitus (IDDM) (45). In this case, $CD8^+$ cells, rather than $CD4^+$ cells, are also suggested to be involved in the apoptosis of β cells in the pancreatic Langerhans islands (46, 47). In both cases, IFN-γ is involved in the pathogenesis of the diseases (48, 49) (50). Thus, these observations indicate that these two types of inflammatory responses are clearly different; EAE and CIA are IL-17 dependent, and IL-17-producing cells play a major role, while IDDM and GVHR are IFN-γ dependent, and $CD8^+$ cytotoxic T cells and/or $CD4^+$ Th1 cells play important roles.

Taken together, our data demonstrate that IL-17 and IFN-γ, produced by a distinct population of T cells, have different roles in the development of EAE, CIA, GVHR, and hyperglycemia. These results suggest that these cytokines may also be involved in the development of MS, RA, GVHD, and IDDM in humans. Elucidation of the roles of pathogenic cytokines and the mechanisms of cytokine dependency may provide potential targets for novel therapeutics to treat these diseases.

Acknowledgments

We thank Dr. S. J. Galli (Stanford University School of Medicine, Stanford, CA) for his generous support for this study. We also thank Tomoko Hata and Hayato Kotaki for their excellent animal care.

Disclosures

The authors have no financial conflict of interest.

References

1. Moseley, T. A., D. R. Haudenschild, L. Rose, and A. H. Reddi. 2003. Interleukin-17 family and IL-17 receptors. *Cytokine Growth Factor Rev.* 14: 155–174.
2. Chabaud, M., J. M. Durand, N. Buchs, F. Fossiez, G. Page, L. Frappart, and P. Miossec. 1999. Human interleukin-17: A T cell-derived proinflammatory cytokine produced by the rheumatoid synovium. *Arthritis Rheum.* 42: 963–970.
3. Wong, C. K., C. Y. Ho, E. K. Li, and C. W. Lam. 2000. Elevation of proinflammatory cytokine (IL-18, IL-17, IL-12) and Th2 cytokine (IL-4) concentrations in patients with systemic lupus erythematosus. *Lupus* 9: 589–593.
4. Hamzaoui, K., A. Hamzaoui, F. Guemira, M. Bessioud, M. Hamza, and K. Ayed. 2002. Cytokine profile in Behcet's disease patients: relationship with disease activity. *Scand. J. Rheumatol.* 31: 205–210.
5. Antonysamy, M. A., W. C. Fanslow, F. Fu, W. Li, S. Qian, A. B. Troutt, and A. W. Thomson. 1999. Evidence for a role of IL-17 in organ allograft rejection: IL-17 promotes the functional differentiation of dendritic cell progenitors. *J. Immunol.* 162: 577–584.
6. Matsumoto, K., and K. Kanmatsuse. 2002. Increased urinary excretion of interleukin-17 in nephrotic patients. *Nephron* 91: 243–249.
7. Wong, C. K., C. Y. Ho, F. W. Ko, C. H. Chan, A. S. Ho, D. S. Hui, and C. W. Lam. 2001. Proinflammatory cytokines (IL-17, IL-6, IL-18 and IL-12) and Th cytokines (IFN-γ, IL-4, IL-10 and IL-13) in patients with allergic asthma. *Clin. Exp. Immunol.* 125: 177–183.
8. Lock, C., G. Hermans, R. Pedotti, A. Brendolan, E. Schadt, H. Garren, A. Langer-Gould, S. Strober, B. Cannella, J. Allard, et al. 2002. Gene-microarray analysis of multiple sclerosis lesions yields new targets validated in autoimmune encephalomyelitis. *Nat. Med.* 8: 500–508.
9. Nakae, S., Y. Komiyama, A. Nambu, K. Sudo, M. Iwase, I. Homma, K. Sekikawa, M. Asano, and Y. Iwakura. 2002. Antigen-specific T cell sensitization is impaired in IL-17-deficient mice, causing suppression of allergic cellular and humoral responses. *Immunity* 17: 375–387.
10. Nakae, S., A. Nambu, K. Sudo, and Y. Iwakura. 2003. Suppression of immune induction of collagen-induced arthritis in IL-17-deficient mice. *J. Immunol.* 171: 6173–6177.
11. Nakae, S., S. Saijo, R. Horai, K. Sudo, S. Mori, and Y. Iwakura. 2003. IL-17 production from activated T cells is required for the spontaneous development of destructive arthritis in mice deficient in IL-1 receptor antagonist. *Proc. Natl. Acad. Sci. USA* 100: 5986–5990.
12. Ye, P., F. H. Rodriguez, S. Kanaly, K. L. Stocking, J. Schurr, P. Schwarzenberger, P. Oliver, W. Huang, P. Zhang, J. Zhang, et al. 2001. Requirement of interleukin 17 receptor signaling for lung CXC chemokine and granulocyte colony-stimulating factor expression, neutrophil recruitment, and host defense. *J. Exp. Med.* 194: 519–527.
13. Aarvak, T., M. Chabaud, P. Miossec, and J. B. Natvig. 1999. IL-17 is produced by some proinflammatory Th1/Th0 cells but not by Th2 cells. *J. Immunol.* 162: 1246–1251.
14. Albanesi, C., C. Scarponi, A. Cavani, M. Federici, F. Nasorri, and G. Girolomoni. 2000. Interleukin-17 is produced by both Th1 and Th2 lymphocytes, and modulates interferon-γ- and interleukin-4-induced activation of human keratinocytes. *J. Invest. Dermatol.* 115: 81–87.
15. Infante-Duarte, C., H. F. Horton, M. C. Byrne, and T. Kamradt. 2000. Microbial lipopeptides induce the production of IL-17 in Th cells. *J. Immunol.* 165: 6107–6115.

173

16. Molet, S., Q. Hamid, F. Davoine, E. Nutku, R. Taha, N. Page, R. Olivenstein, J. Elias, and J. Chakir. 2001. IL-17 is increased in asthmatic airways and induces human bronchial fibroblasts to produce cytokines. *J. Allergy Clin. Immunol.* 108: 430–438.
17. Ferretti, S., O. Bonneau, G. R. Dubois, C. E. Jones, and A. Trifilieff. 2003. IL-17, produced by lymphocytes and neutrophils, is necessary for lipopolysaccharide-induced airway neutrophilia: IL-15 as a possible trigger. *J. Immunol.* 170: 2106–2112.
18. Happel, K. I., M. Zheng, E. Young, L. J. Quinton, E. Lockhart, A. J. Ramsay, J. E. Shellito, J. R. Schurr, G. J. Bagby, S. Nelson, and J. K. Kolls. 2003. Roles of Toll-like receptor 4 and IL-23 in IL-17 expression in response to *Klebsiella pneumoniae* infection. *J. Immunol.* 170: 4432–4436.
19. Matusevicius, D., P. Kivisakk, B. He, N. Kostulas, V. Ozenci, S. Fredrikson, and H. Link. 1999. Interleukin-17 mRNA expression in blood and CSF mononuclear cells is augmented in multiple sclerosis. *Mult. Scler.* 5: 101–104.
20. Zhang, G. X., B. Gran, S. Yu, J. Li, I. Siglienti, X. Chen, M. Kamoun, and A. Rostami. 2003. Induction of experimental autoimmune encephalomyelitis in IL-12 receptor-β2-deficient mice: IL-12 responsiveness is not required in the pathogenesis of inflammatory demyelination in the central nervous system. *J. Immunol.* 170: 2153–2160.
21. Kassiotis, G., K. Kranidioti, and G. Kollias. 2001. Defective CD4T cell priming and resistance to experimental autoimmune encephalomyelitis in TNF-deficient mice due to innate immune hypo-responsiveness. *J. Neuroimmunol.* 119: 239–247.
22. Ferber, I. A., S. Brocke, C. Taylor-Edwards, W. Ridgway, C. Dinisco, L. Steinman, D. Dalton, and C. G. Fathman. 1996. Mice with a disrupted IFN-γ gene are susceptible to the induction of experimental autoimmune encephalomyelitis (EAE). *J. Immunol.* 156: 5–7.
23. Willenborg, D. O., S. Fordham, C. C. Bernard, W. B. Cowden, and I. A. Ramshaw. 1996. IFN-γ plays a critical down-regulatory role in the induction and effector phase of myelin oligodendrocyte glycoprotein-induced autoimmune encephalomyelitis. *J. Immunol.* 157: 3223–3227.
24. Chu, C. Q., S. Wittmer, and D. K. Dalton. 2000. Failure to suppress the expansion of the activated CD4 T cell population in interferon γ-deficient mice leads to exacerbation of experimental autoimmune encephalomyelitis. *J. Exp. Med.* 192: 123–128.
25. Krakowski, M., and T. Owens. 1996. Interferon-γ confers resistance to experimental allergic encephalomyelitis. *Eur. J. Immunol.* 26: 1641–1646.
26. Langrish, C. L., Y. Chen, W. M. Blumenschein, J. Mattson, B. Basham, J. D. Sedgwick, T. McClanahan, R. A. Kastelein, and D. J. Cua. 2005. IL-23 drives a pathogenic T cell population that induces autoimmune inflammation. *J. Exp. Med.* 201: 233–240.
27. Traugott, U., and P. Lebon. 1988. Demonstration of α, β, and γ interferon in active chronic multiple sclerosis lesions. *Ann. NY Acad. Sci.* 540: 309–311.
28. Hammarberg, H., O. Lidman, C. Lundberg, S. Y. Eltayeb, A. W. Gielen, S. Muhallab, A. Svenningsson, H. Linda, P. H. van Der Meide, S. Cullheim, et al. 2000. Neuroprotection by encephalomyelitis: rescue of mechanically injured neurons and neurotrophin production by CNS-infiltrating T and natural killer cells. *J. Neurosci.* 20: 5283–5291.
29. Begolka, W. S., and S. D. Miller. 1998. Cytokines as intrinsic and exogenous regulators of pathogenesis in experimental autoimmune encephalomyelitis. *Res. Immunol.* 149: 771–781; discussion 843; 774; 855–760.
30. Becher, B., B. G. Durell, and R. J. Noelle. 2002. Experimental autoimmune encephalitis and inflammation in the absence of interleukin-12. *J. Clin. Invest.* 110: 493–497.
31. Gran, B., G. X. Zhang, S. Yu, J. Li, X. H. Chen, E. S. Ventura, M. Kamoun, and A. Rostami. 2002. IL-12p35-deficient mice are susceptible to experimental autoimmune encephalomyelitis: evidence for redundancy in the IL-12 system in the induction of central nervous system autoimmune demyelination. *J. Immunol.* 169: 7104–7110.
32. Park, H., Z. Li, X. O. Yang, S. H. Chang, R. Nurieva, Y. H. Wang, Y. Wang, L. Hood, Z. Zhu, Q. Tian, and C. Dong. 2005. A distinct lineage of CD4 T cells regulates tissue inflammation by producing interleukin 17. *Nat. Immunol.* 6: 1133–1141.
33. Harrington, L. E., R. D. Hatton, P. R. Mangan, H. Turner, T. L. Murphy, K. M. Murphy, and C. T. Weaver. 2005. Interleukin 17-producing $CD4^+$ effector T cells develop via a lineage distinct from the T helper type 1 and 2 lineages. *Nat. Immunol.* 6: 1123–1132.
34. Aggarwal, S., N. Ghilardi, M. H. Xie, F. J. de Sauvage, and A. L. Gurney. 2003. Interleukin-23 promotes a distinct CD4 T cell activation state characterized by the production of interleukin-17. *J. Biol. Chem.* 278: 1910–1914.
35. Umemura, M., T. Kawabe, K. Shudo, H. Kidoya, M. Fukui, M. Asano, Y. Iwakura, G. Matsuzaki, R. Imamura, and T. Suda. 2004. Involvement of IL-17 in Fas ligand-induced inflammation. *Int. Immunol.* 16: 1099–1108.
36. Xiao, B. G., C. Linington, and H. Link. 1991. Antibodies to myelin-oligodendrocyte glycoprotein in cerebrospinal fluid from patients with multiple sclerosis and controls. *J. Neuroimmunol.* 31: 91–96.
37. Sun, J., H. Link, T. Olsson, B. G. Xiao, G. Andersson, H. P. Ekre, C. Linington, and P. Diener. 1991. T and B cell responses to myelin-oligodendrocyte glycoprotein in multiple sclerosis. *J. Immunol.* 146: 1490–1495.
38. Ichikawa, M., T. G. Johns, J. Liu, and C. C. Bernard. 1996. Analysis of the fine B cell specificity during the chronic/relapsing course of a multiple sclerosis-like disease in Lewis rats injected with the encephalitogenic myelin oligodendrocyte glycoprotein peptide 35–55. *J. Immunol.* 157: 919–926.
39. Wolf, S. D., B. N. Dittel, F. Hardardottir, and C. A. Janeway, Jr. 1996. Experimental autoimmune encephalomyelitis induction in genetically B cell-deficient mice. *J. Exp. Med.* 184: 2271–2278.
40. Hjelmstrom, P., A. E. Juedes, J. Fjell, and N. H. Ruddle. 1998. B-cell-deficient mice develop experimental allergic encephalomyelitis with demyelination after myelin oligodendrocyte glycoprotein sensitization. *J. Immunol.* 161: 4480–4483.
41. Dittel, B. N., T. H. Urbania, and C. A. Janeway, Jr. 2000. Relapsing and remitting experimental autoimmune encephalomyelitis in B cell deficient mice. *J. Autoimmun.* 14: 311–318.
42. Hunter, S. F., D. J. Miller, and M. Rodriguez. 1997. Monoclonal remyelination-promoting natural autoantibody SCH 94.03: pharmacokinetics and in vivo targets within demyelinated spinal cord in a mouse model of multiple sclerosis. *J. Neurol. Sci.* 150: 103–113.
43. Baker, M. B., N. H. Altman, E. R. Podack, and R. B. Levy. 1996. The role of cell-mediated cytotoxicity in acute GVHD after MHC-matched allogeneic bone marrow transplantation in mice. *J. Exp. Med.* 183: 2645–2656.
44. Brochu, S., B. Rioux-Masse, J. Roy, D. C. Roy, and C. Perreault. 1999. Massive activation-induced cell death of alloreactive T cells with apoptosis of bystander postthymic T cells prevents immune reconstitution in mice with graft-versus-host disease. *Blood* 94: 390–400.
45. Vukkadapu, S. S., J. M. Belli, K. Ishii, A. G. Jegga, J. J. Hutton, B. J. Aronow, and J. D. Katz. 2005. Dynamic interaction between T cell-mediated β cell damage and β cell repair in the run-up to autoimmune diabetes of the NOD mouse. *Physiol. Genomics* 21: 201–211.
46. Kagi, D., B. Odermatt, P. Seiler, R. M. Zinkernagel, T. W. Mak, and H. Hengartner. 1997. Reduced incidence and delayed onset of diabetes in perforin-deficient nonobese diabetic mice. *J. Exp. Med.* 186: 989–997.
47. Itoh, N., A. Imagawa, T. Hanafusa, M. Waguri, K. Yamamoto, H. Iwahashi, M. Moriwaki, H. Nakajima, J. Miyagawa, M. Namba, et al. 1997. Requirement of Fas for the development of autoimmune diabetes in nonobese diabetic mice. *J. Exp. Med.* 186: 613–618.
48. Hultgren, B., X. Huang, N. Dybdal, and T. A. Stewart. 1996. Genetic absence of γ-interferon delays but does not prevent diabetes in NOD mice. *Diabetes* 45: 812–817.
49. Wang, B., I. Andre, A. Gonzalez, J. D. Katz, M. Aguet, C. Benoist, and D. Mathis. 1997. Interferon-γ impacts at multiple points during the progression of autoimmune diabetes. *Proc. Natl. Acad. Sci. USA* 94: 13844–13849.
50. Ellison, C. A., J. M. Fischer, K. T. HayGlass, and J. G. Gartner. 1998. Murine graft-versus-host disease in an F_1-hybrid model using IFN-γ gene knockout donors. *J. Immunol.* 161: 631–640.

Signaling of vascular endothelial growth factor receptor-1 tyrosine kinase promotes rheumatoid arthritis through activation of monocytes/macrophages

Masato Murakami, Shinobu Iwai, Sachie Hiratsuka, Mai Yamauchi, Kazuhide Nakamura, Yoichiro Iwakura, and Masabumi Shibuya

Vascular endothelial growth factor (VEGF) and VEGF receptor-1 (VEGFR-1/Flt-1) were shown to be involved in pathological angiogenesis, particularly rheumatoid arthritis (RA). However, the molecular basis of their actions is not fully understood. Here we report that in a murine model of RA, deletion of the tyrosine kinase (TK) domain of VEGFR-1 decreased the incidence and clinical symptoms of RA. Pathological symptoms, such as synovial hyperplasia, inflammatory infiltrates, pannus formation, and cartilage/bone destruction, became milder in *Vegfr-1 tk$^{-/-}$* mice compared with wild-type (Wt) mice in the human T-cell leukemia virus-1 *(HTLV-1) pX*–induced chronic models. VEGFR-1 TK-deficient bone marrow cells showed a suppression of multilineage colony formation. Furthermore, macrophages induced to differentiate in vitro showed a decrease in immunologic reactions such as phagocytosis and the secretion of interleukin-6 (IL-6) and VEGF-A. Treatment of this RA model with a small molecule inhibitor for VEGFR TK, KRN951, also attenuated the arthritis. These results indicate that the VEGFR-1 TK signaling modulates the proliferation of bone marrow hematopoietic cells and immunity of monocytes/macrophages and promotes chronic inflammation, which may be a new target in the treatment of RA. (Blood. 2006;108:1849-1856)

© 2006 by The American Society of Hematology

Introduction

Vascular endothelial growth factors (VEGFs) and their receptors (VEGFRs), including VEGFR-1 (Flt-1), VEGFR-2 (KDR/Flk-1), and VEGFR-3 (Flt-4), form a regulatory system crucial for normal development and pathological angiogenesis.[1-4] VEGFRs are structurally related to the Fms/Kit/PDGFR family and contain an extracellular domain carrying 7 immunoglobulin (Ig)–like repeats and a cytoplasmic tyrosine kinase (TK) domain.[5,6] VEGFR-1 and VEGFR-2 are highly expressed on vascular endothelial cells.[7-10] We and others have recently shown that VEGFR-1 is expressed not only in vascular endothelial cells but also in monocytes/macrophages,[11,12] and its signaling is involved in the migration of macrophages toward VEGF-A.[13] In addition to VEGF-A, VEGF-B and PlGF are also ligands for VEGFR-1; thus, they could play a role in this signaling under both physiological and pathological conditions. Other nonendothelial cells, including smooth muscle cells, trophoblasts, and osteoblasts, were reported to express VEGFR-1.[14]

Mice lacking *Vegfr-2* die in the embryonic stage due to a severe deficiency of vascular development.[15] In contrast, mice lacking *Vegfr-1* die due to overgrowth and disorganization of the vascular system.[16] Interestingly, however, mouse embryos lacking the TK domain of *Vegfr-1* survive without significant defects,[17] suggesting that VEGFR-1 functions as a negative regulator of vascular development by trapping VEGF-A via its ligand-binding domain.[14] Recently, various studies including ours indicated that the expression of VEGFs and VEGFRs is up-regulated in various diseases.[2,4,18-20] VEGFR-1–mediated signaling was shown to play a significant role in a variety of pathological conditions such as carcinogenesis and inflammatory diseases.[19,21,22] VEGFR-1 signaling facilitates tumor angiogenesis and spontaneous lung metastases by inducing the expression of matrix metalloproteinase 9 (MMP-9).[22-24] A recent study also showed that VEGFR-1 is important for the reconstitution of hematopoiesis in bone marrow (BM) after irradiation.[25]

Rheumatoid arthritis (RA)[26] is a chronic systemic disease characterized by an inflammatory erosive synovitis, which shows marked neovascularization, inflammatory cell infiltration, and synovial hyperplasia. These pathological reactions gradually induce a pannus, with inflammatory vascular tissue leading to an irreversible loss of cartilage and bone.[27,28] VEGF-A is highly expressed in synovial fluid in RA.[29] Immunohistochemical and in situ hybridization studies on the synovial tissues have shown that VEGF-A is strongly expressed in synovial macrophages, fibroblasts surrounding microvessels, and vascular smooth muscle cells.[29,30] In inflamed joints, many cytokines, including VEGF and the proinflammatory interleukin-1 (IL-1), IL-6, and tumor

From the Division of Genetics and Division of Cell Biology, Center for Experimental Medicine, Institute of Medical Science, University of Tokyo, Japan; Department of Pharmacology, Tokyo Women's Medical University, Japan; and Pharmaceutical Developmental Laboratories, Kirin Brewery, Gunma, Japan.

Submitted December 21, 2005; accepted May 1, 2006. Prepublished online as *Blood* First Edition Paper, May 18, 2006; DOI 10.1182/blood-2006-04-016030.

Supported by Grant-in-Aid Special Project Research on Cancer-Bioscience 12215024 from the Ministry of Education, Culture, Sports, Science and Technology in Japan; a grant for the program "Research for the Future" from the Japan Society for Promotion of Science; and the program "Promotion of Fundamental Research in Health Science" from the Organization for Pharmaceutical Safety and Research (OPSR).

M.M., Y.I., and M.S. participated in designing the research; M.M., S.I., and M.Y. performed the research; M.M. centralized the pathological review and analyzed data; S.H. and Y.I provided gene-targeting mice; K.N. provided new reagents; M.M. and M.S. wrote the manuscript; and all authors checked the final version of the manuscript.

The online version of the article contains a data supplement.

Reprints: Masabumi Shibuya, Division of Genetics, Institute of Medical Science, University of Tokyo, 4-6-1, Shirokane-dai, Minato-ku, Tokyo, 108-8639, Japan; e-mail: shibuya@ims.u-tokyo.ac.jp.

The publication costs of this article were defrayed in part by page charge payment. Therefore, and solely to indicate this fact, this article is hereby marked "advertisement" in accordance with 18 U.S.C. section 1734.

© 2006 by The American Society of Hematology

necrosis factor-α (TNF-α), play important roles in the pathogenesis of RA.[31]

Iwakura et al have recently reported that the human T-cell leukemia virus-1 *(HTLV-1) pX* transgenic mouse is a useful model for studying RA[32] in that it is more similar to human RA than other models, such as collagen-antibody–induced arthritis, in terms of chronic progression, the production of rheumatoid factor, and pathological findings.[33] Interesting characteristics of *pX* transgenic mice include a high incidence of arthritis in the BALB/c genetic background[34] and up-regulation of the production of cytokines such as IL-6 and TNF-α.[35] However, it is not clear yet how the signaling of VEGFR-1 is involved in *pX*-induced or anticollagen-antibody–induced RA.

In this study, we examined these points using wild-type and *Vegfr-1 tk*–deficient mice. We have found that in *Vegfr-1* $tk^{-/-}$ mice, the arthritis was significantly suppressed through a decrease in the inflammatory response of monocytes/macrophages and hematopoietic proliferation.

Materials and methods

Mice and the marker-assisted selection protocol (MASP)

All the experiments using animal models were carried out according to the guidelines set by the Animal Center of The Institute of Medical Science, The University of Tokyo. To obtain *Vegfr-1* $tk^{-/-}$ mice with the BALB/c background, we backcrossed *Vegfr-1* $tk^{+/-}$ heterozygous males (original genetic background is 50% 129SV and 50% C57BL/6) with BALB/c females using marker-assisted selection protocol (MASP) (speed congenics). First, a total of 60 polymorphic polymerase chain reaction (PCR)–based microsatellite loci were randomly obtained from Mouse Genome Informatics of The Jackson Laboratory[36] (Table S1, available on the *Blood* website; see the Supplemental Materials link at the top of the online article). Two to 6 markers were set for each chromosome with an average spacing of 20 cM. At every generation, the mouse carrying the fewest C57BL/6 background loci was used for backcrossing. After 4 generations, less than 3% of C57BL/6 background loci were left, and then crosses were made with *pX* transgenic mice to compare the incidence of arthritis in newly prepared congenic mice with that in the control *pX* mice. Finally, *pX Vegfr-1* $tk^{+/-}$ mice were crossed with *Vegfr-1* $tk^{+/-}$ mice for the experiments (Figure 1B).

For the *pX*-induced arthritis, animals were observed every month from age 2 to 6 months and then killed for assessment. For the collagen-antibody–induced arthritis, 8-week-old BALB/c female *Vegfr-1* $tk^{-/-}$ and wild-type mice were used. Acute arthritis was induced by the intraperitoneal injection of 1 mg of an antitype II collagen–monoclonal antibody cocktail (Chondrex, Redmond, WA) on day 0 followed by the intraperitoneal injection of 50 μg lipopolysaccharide (LPS) on day 3. Animals were killed for assessment on day 7.

Arthritis and histologic score

The incidence and severity of arthritis were examined monthly for *pX* mice and daily for mice with collagen-antibody–induced arthritis by qualitative clinical scoring as follows: 0, normal; 1, mild redness and swelling of the ankle or wrist; 2, moderate redness and swelling; 3, severe redness and swelling of the entire paw; 4, maximally inflamed limb within multiple joints. The number of joints observed was 33 to 122 for each genotype and each month. Mice were killed by neck dislocation, and joints were fixed in paraformaldehyde (PFA) and decalcified in EDTA. Then sagittal paw paraffin sections were examined by hematoxylin and eosin (HE) staining and immunohistochemical staining with von Willebrand factor (VWF) antibody (Dakopatts, Glostrup, Denmark). Histologic examination including morphologic analysis was carried out by semiquantitive grade scoring. In brief, for each paw joint, synovial hyperplasia, inflammatory cell infiltration, pannus formation, and bone and cartilage destruction were scored as follows: 0, none; 1, mild; 2, moderate; 3, severe. The sum of the scores for each paw was used as a histologic score index of the 64 paws for *pX* mice and 50 paws for *pX Vegfr-1* $tk^{-/-}$ mice. The density of VWF-positive vessels in the hyperplasic synovia was determined by measuring the immunoreactive area in 3 chosen paw joints, which had an average grade. Vascular density was analyzed using a Kurabo Angiogenesis Image Analyzer (Kurabo, Osaka, Japan).

Macrophage activities for cytokine secretion and phagocytosis

For the cytokine secretion assay, mouse peritoneal macrophages were collected 3 days after the intraperitoneal injection of 4% thioglycolate. Peritoneal lavage was collected with 0.5% BSA, 2 mM EDTA (pH 7.2), and PBS, washed twice, and purified using anti-mouse CD11b magnetic-activated cell sorting (MACS) (Miltenyi Biotec, Bergisch Gladbach, Germany). The purity of macrophages was more than 90%. About 4×10^5 macrophages in 0.2 mL of 0.1% BSA–RPMI 1640 medium were seeded into a 96-well plate and incubated with recombinant human VEGF-A (hVEGF-A) (100 ng/mL) or control PBS, with or without a VEGFR inhibitor, SU5416[37] or KRN633.[38] After 48 hours of incubation, the supernatants were collected after centrifugation and cytokine concentrations were measured using a mouse IL-6 and VEGF-A enzyme-linked immunosorbent assay (ELISA) kit (R&D Systems, Minneapolis, MN). Total RNA from hVEGF-A–stimulated macrophages after 24 hours of incubation was isolated using an RNeasy Quick spin column (QIAGEN, Hilden, Germany). The total RNA was analyzed using a real-time reverse transcriptase (RT)–PCR according to the manufacturer's instructions (Takara Bio, Shiga, Japan). All the primers used for the amplification are listed in Table S2. For the phagocytosis assay, BM mononuclear cells (BMMNCs) of both *Vegfr-1* $tk^{-/-}$ and wild-type mice were collected from the femur, and then 3×10^6 cells in 3.0 mL were cultured in 6-well plates with 100 ng/mL M-CSF (R&D Systems) in 10% FCS–RPMI 1640 medium. On days 2 and 5 of culture, nonadherent cells were discarded. On day 7, the confluent monolayers of adherent macrophages were used for the phagocytosis assay. Confluent macrophages were washed twice with cold PBS, resuspended in 1 mL RPMI 1640 medium containing FITC-dextran (Sigma, St Louis, MO) (100 ng/mL) or Alexa LPS (20 ng/mL) (Molecular Probes, Eugene, OR), and incubated for 2 hours at 37°C. After the incubation, plates were immediately transferred onto ice. This was followed by a quick aspiration of the medium and the washing of cells to remove unphagocytosed particles. Adding PFA stopped the phagocytotic reaction. Total fluorescence was measured with a fluorescence-activated cell sorting (FACS) machine Epics-XL (Beckman Coulter, Fullerton CA). The instrument was set to collect 2×10^4 cells, and profiles of phagocytosis were analyzed using FlowJo software (Tree Star, Ashland, OR).

Treatment of arthritis-model mice with a kinase inhibitor

A low-molecular-weight chemical, KRN951, was obtained from the Kirin Brewery (Gunma, Japan). KRN951 is a VEGFR inhibitor suppressing the TK of VEGFR-1, VEGFR-2, and VEGFR-3. Inhibition of the phosphorylation of VEGFR-1 and -2 with KRN951 is shown in Figure S1. KRN951 was dissolved in 0.5% methylcellulose, Metolose SM15 (Shin-Etsu Chemical, Tokyo, Japan). The KRN951 solution was orally administered to mice with *pX*-induced arthritis at 20 mg/kg/d for 5 days a week, with a 2-day rest period, between the age of 8 and 26 weeks. The mice with collagen-antibody–induced arthritis were given the same inhibitor from day 3 to day 7 at 10, 20, and 40 mg/kg/d, respectively. The control solution was 0.5% methylcellulose without the inhibitor.

Colony formation assay

About 1×10^5 BMMNCs per 35-mm plate (triplicate) were cultured in complete methylcellulose containing 50 ng/mL recombinant murine SCF (rmSCF), 10 ng/mL rmIL-3, 10 ng/mL rhIL-6, and 3 U/mL recombinant human erythropoietin (rhEPO) (Stem Cell Technologies, Vancouver, BC, Canada). Colonies were scored and phenotyped on an inverted phase microscope 10 days after seeding.

Flow cytometric analysis of BM cells

Mouse BM cells were isolated by flushing the femur BM tissues with 1% FBS–PBS, and a single-cell suspension was obtained. Remaining red blood cells were removed with lysis buffer (10 mM NH_4Cl). BMMNCs were stained with monoclonal antibodies for Sca-1 (BD Pharmingen, San Diego, CA) and CD34 (BD Pharmingen) and analyzed using a flow cytometer (Epics-XL, Beckman Coulter). The instrument was set to collect 2×10^4 cells, and these cells were analyzed using FlowJo software (Tree Star). All experiments were performed in triplicate.

Statistical analysis

An unpaired Student *t* test was used for all analyses. Differences were considered to be statistically significant for *P* values below .05 and .01.

Results

Speed congenics significantly shorten the period of backcrossing for establishing *Vegfr-1 tk*$^{-/-}$ BALB/c mice

The incidence of arthritis in *pX* transgenic mice is significantly higher in the genetic background of BALB/c than C57BL/6. Because the original genetic background of *Vegfr-1 tk*$^{-/-}$ mice is 50% 129SV and 50% C57BL/6, we prepared BALB/c-background congenic mice carrying the *Vegfr-1 tk*$^{+/-}$ gene. To shorten the crossing time, we used a MASP or speed congenics to establish BALB/c congenic mice (see "Materials and methods"). The mouse showing the least number of C57BL/6-background loci was selected for backcrossing. After 4 generations, less than 3% of the C57BL/6 background was left (Figure 1A). After the speed congenics, *Vegfr-1 tk*$^{+/-}$ BALB/c congenic mice were mated with *pX* BALB/c mice, which generated 4 genotypes (*pX*, *pX Vegfr-1*$^{+/-}$, *Vegfr-1*$^{+/-}$, and wild-type) (Figure 1B).

To confirm that the congenic strain efficiently changed to the BALB/c background, we compared the incidence of arthritis between the original *pX* mice and the newly prepared congenic *pX* mice. The original *pX* mice and the speed congenic BALB/c *pX* mice showed severe arthritis with no difference in the incidence of disease (Figure 1C). After verification, we mated *pX Vegfr-1 tk*$^{+/-}$ and *Vegfr-1 tk*$^{+/-}$ mice to generate the transgenic mice and other mice for the experiments (Figure 1B).

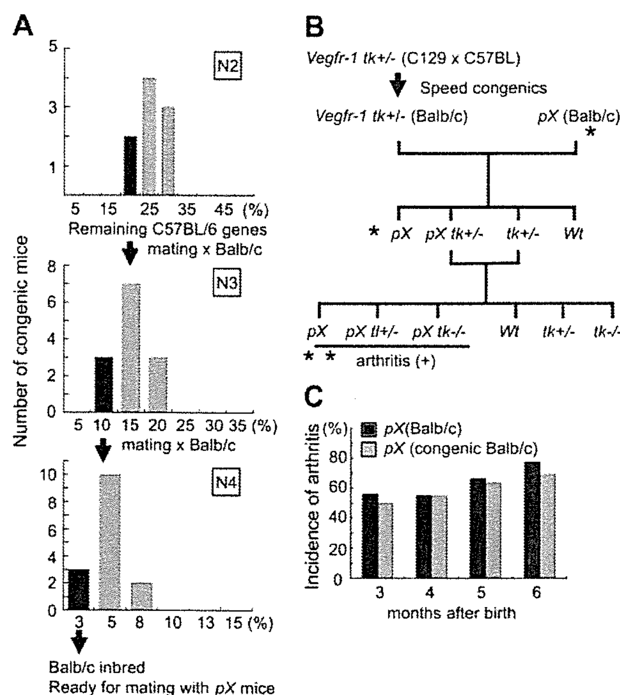

Figure 1. Experimental design and speed congenics used to shorten the period of backcrossing. (A) Percentage of the C57BL/6 polymorphism loci remaining in the backcrossed generation of mice. After 4 generations, a few mice had less than 3% of C57BL/6 background loci. (B) Experimental design for *pX*-induced RA in the *Vegfr-1 tk*$^{-/-}$ background. *Confirmation of the incidence of arthritis in newly prepared BALB/c speed congenic *pX* and original BALB/c *pX* transgenic mice. **The incidence and degree of arthritis in these mice were examined. (C) Comparison of the incidence of arthritis between newly prepared BALB/c speed congenic *pX* transgenic mice and original BALB/c *pX* transgenic mice. No difference was observed during the first 3 to 6 months after birth.

Signals from VEGFR-1 TK contribute to the onset and the progression of arthritis

We measured the incidence and clinical grade of arthritis in the presence or absence of VEGFR-1 TK signals using *pX*, *pX Vegfr-1 tk*$^{+/-}$, and *pX Vegfr-1 tk*$^{-/-}$ mice (Figure 1B). The incidence of arthritis, detected as paw swelling, erythema, and ankylosis, was significantly lower in *pX Vegfr-1 tk*$^{-/-}$ mice than *Vegfr-1* wild-type *pX* transgenic mice at all the stages examined ($P < .072$ at 2 to 6 months) (Figure 2A). In addition, the incidence of arthritis was lower in the heterozygous *Vegfr-1 tk*$^{+/-}$ mice than *pX* transgenic wild-type mice before 4 months of age, although the difference was not statistically significant (Figure 2A). Clinical scores measured based on redness and swelling of the ankle or wrist were also significantly lower in *pX Vegfr-1 tk*$^{-/-}$ mice than *pX* wild-type mice ($P < .058$ at 2 to 6 months). Furthermore, *pX Vegfr-1 tk*$^{+/-}$ mice showed mild clinical scores between those of *pX* mice and *pX Vegfr-1 tk*$^{-/-}$ mice ($P = .025$ to .454 at 2 to 6 months) (Figure 2B).

Next we examined the histologic difference between *pX* mice and *pX Vegfr-1 tk*$^{-/-}$ mice. Synovial hyperplasia, inflammatory infiltrates, pannus formation, and loss of cartilage/bone were reduced by about half in *pX Vegfr-1 tk*$^{-/-}$ mice compared with *pX* wild-type mice ($P = .015$, .011, .007, and .026, respectively) (Figure 2F). Typical histologic findings are shown in Figure 2C-E.

Because VEGFR-1 is considered to be associated with angiogenesis, we examined capillary formation in the pannus of synovial tissue. Capillary densities were about 17% lower in *pX Vegfr-1 tk*$^{-/-}$ mice than *pX* wild-type mice; however, the difference was not significant ($P = .623$) (Figure 3A-C). These results suggest that VEGFR-1 TK–dependent signals contribute to the symptoms of arthritis, including pathological findings, in a gene-dosage–dependent manner.

Production of cytokines by monocytes/macrophages and the function of these cells are important for arthritis

We and others already showed that VEGFR-1 is expressed on monocytes/macrophages[12,13] and that the VEGF-dependent migration of macrophages is suppressed in *Vegfr-1 tk*$^{-/-}$ mice.[17] Therefore, we examined local infiltration and the functions of monocytes/macrophages in these mice. The infiltration of inflammatory cells into arthritic joints was significantly less extensive in *pX Vegfr-1 tk*$^{-/-}$ mice than in *pX* wild-type mice (Figure 2D-F). We also observed using real-time RT-PCR that angiogenic factors and proinflammatory cytokines are up-regulated in their expression in inflammatory joints of *pX* transgenic mice compared with wild-type mice (Figure S2).

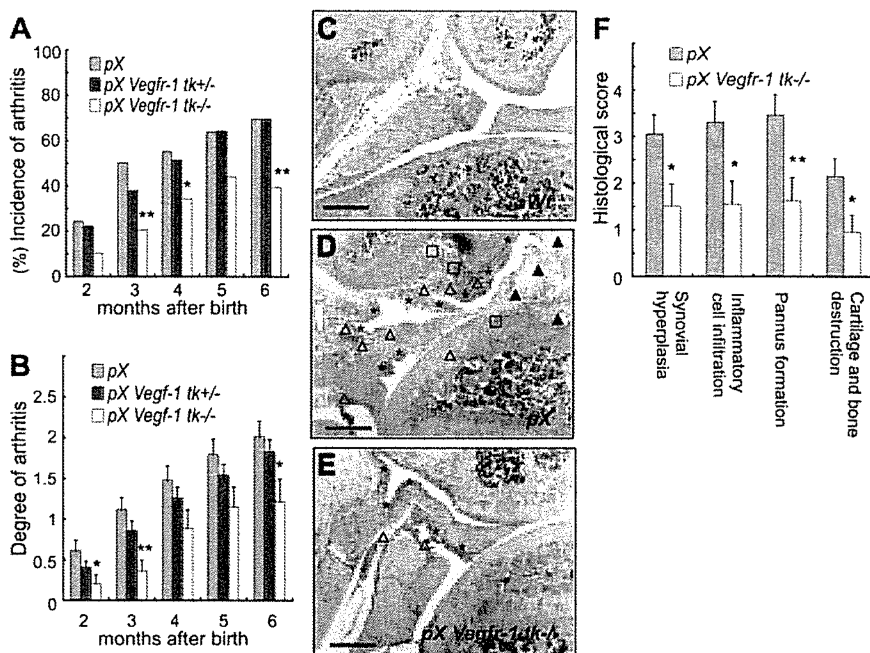

Figure 2. Signals from VEGFR-1 TK contribute to the onset and progression of arthritis. (A) The incidence of arthritis was significantly lower in *pX Vegfr-1 tk*$^{-/-}$ mice than *pX* mice. In addition, the incidence of arthritis in *pX Vegfr-1 tk*$^{+/-}$ heterozygotes was slightly lower in the early stages. (B) Clinical grades of arthritis were reduced depending on the deficiency of the VEGFR-1 TK domain from 2 to 6 months after birth. *pX Vegfr-1 tk*$^{+/-}$ mice showed mild clinical scores between those of *pX* and *pX Vegfr-1 tk*$^{-/-}$ mice. The data (A-B) represent the mean ± SEM obtained from 33 to 122 mice. *$P < .05$ versus *pX*; **$P < .01$ versus *pX*. (C-E) Cross-sections of ankle joints in control and RA mice. Joints of wild-type mice (C) show no remarkable change. Joints of *pX* mice (D) show synovial hyperplasia (*), inflammatory cell infiltration (△), pannus formation (▲), and loss of cartilage and bone (□). These findings are milder in *pX Vegfr-1 tk*$^{-/-}$ mice (E). Sections are taken from average cases in these mice. Scale bars, 200 μm. Images in panels C-E were taken with a Nikon Eclipse TE600 microscope (Nikon, Tokyo, Japan) using AxioVision 3.0 software (Carl Zeiss, Jena, Germany) and a 10×/0.30 NA objective lens, then processed with Photoshop CS (Adobe Systems, San Jose, CA). (F) Histologic scores of the degree of pathology in paws and ankles. Scores of *pX Vegfr-1 tk*$^{-/-}$ mice were about half those of the *pX* mice. The data represent the mean ± SEM. *$P < .05$ versus *pX*; **$P < .01$ versus *pX*.

Secretion of cytokines and phagocytosis are attenuated in *Vegfr-1 tk*$^{-/-}$ macrophages

Saijo et al[39] recently reported that *pX Il-1*$^{-/-}$ mice show a dramatically decreased incidence of arthritis. Because macrophages are an important source of these cytokines, we next focused on the function of macrophages derived from wild-type and *Vegfr-1 tk*–deficient mice. Secretion of IL-6 and VEGF-A was measured in the presence or absence of hVEGF-A. IL-6 was secreted in response to hVEGF-A both in the wild-type and in the *Vegfr-1 tk*$^{-/-}$ mice (Figure 4A). However, much less IL-6 was secreted from *Vegfr-1 tk*$^{-/-}$ macrophages than *Vegfr-1* wild-type cells. In addition, the secretion of IL-6 was partially suppressed with VEGFR inhibitors, SU5416 and KRN633, in the presence of hVEGF-A (Figure 4A).

VEGF-A was secreted from macrophages, and the secretion increased in response to exogenous hVEGF-A (Figure 4B). However, the secretion of VEGF-A from *Vegfr-1 tk*$^{-/-}$ macrophages was about half that in the wild-type mice (Figure 4B).

We examined the mRNA levels of *Il-6* and *Vegf-A* in macrophages in the presence or absence of hVEGF-A by real-time RT-PCR. The expression of both *Il-6* and *Vegf-A* was significantly suppressed in *Vegfr-1 tk*$^{-/-}$ macrophages ($P = .021$ and $< .001$, respectively) (Figure 4C). These results are consistent with the levels of protein determined by ELISA (Figure 4A-B).

Macrophages are multifunctional cells involved in immunologic reactions and phagocytosis. Therefore, we next examined the extent of phagocytosis using macrophages that were induced to differentiate in culture. Wild-type BM-derived and M-CSF–stimulated macrophages efficiently phagocytized both fluorescent dextran and LPS. Surprisingly, however, macrophages from *Vegfr-1 tk*–deficient mice showed significantly less phagocytotic activity (Figure 4D).

Therefore, in addition to the suppression of VEGF-A–dependent migration, *Vegfr-1 tk*-deficient macrophages were dysfunctional in the secretion of IL-6 and VEGF-A as well as phagocytosis under these experimental conditions.

VEGFR TK inhibitor, KRN951, suppressed the progression of arthritis

To confirm the therapeutic effect of VEGFR kinase inhibitors on arthritis, we administered such an inhibitor, KRN951, to mice with *pX*-induced chronic arthritis and collagen-antibody–induced acute arthritis. We treated the mice with KRN951 for 5 straight days (oral, 20 mg/kg/d) a week from 8 to 26 weeks of age (Figure 5A). Administration of KRN951 reduced the progression of arthritis compared with the control ($P < .041$ from 18 weeks to 26 weeks) (Figure 5B). Histologic abnormalities in the treated group decreased 11% to 25% compared with the control (statistically not significant) (Figure 5C). In our preliminary experiments, a dose of KRN951 (1.0 mg/kg body weight) lower than those used in this experiment strongly suppressed the growth of several solid tumors in vivo in mice, suggesting that the dose of KRN951 used here

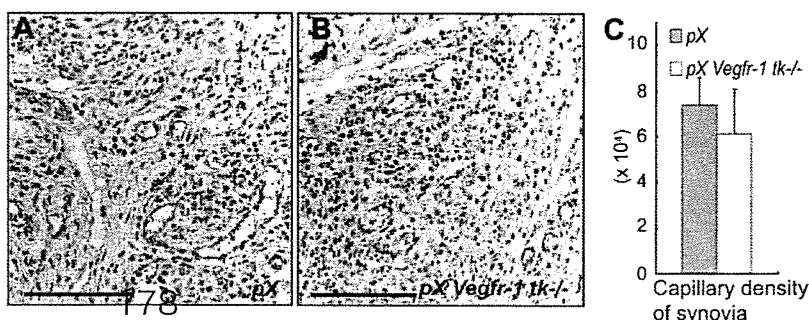

Figure 3. No significant difference was observed in newly formed vessel densities in the hyperplastic synovia and pannus between *pX* mice and *pX Vegfr-1 tk*$^{-/-}$ mice. (A-B) Staining for VWF in the newly formed capillary vessels in the hyperplastic synovia and pannus. Scale bars, 50 μm. Images were taken with a Nikon Eclipse TE600 microscope, using AxioVision 3.0 software and a 40×/0.75 NA objective lens, then processed with Photoshop CS. (C) Vascular densities in the hyperplastic synovia are slightly lower in *pX Vegfr-1 tk*$^{-/-}$ mice than in *pX* mice ($P = .623$). The data represent the mean ± SEM.

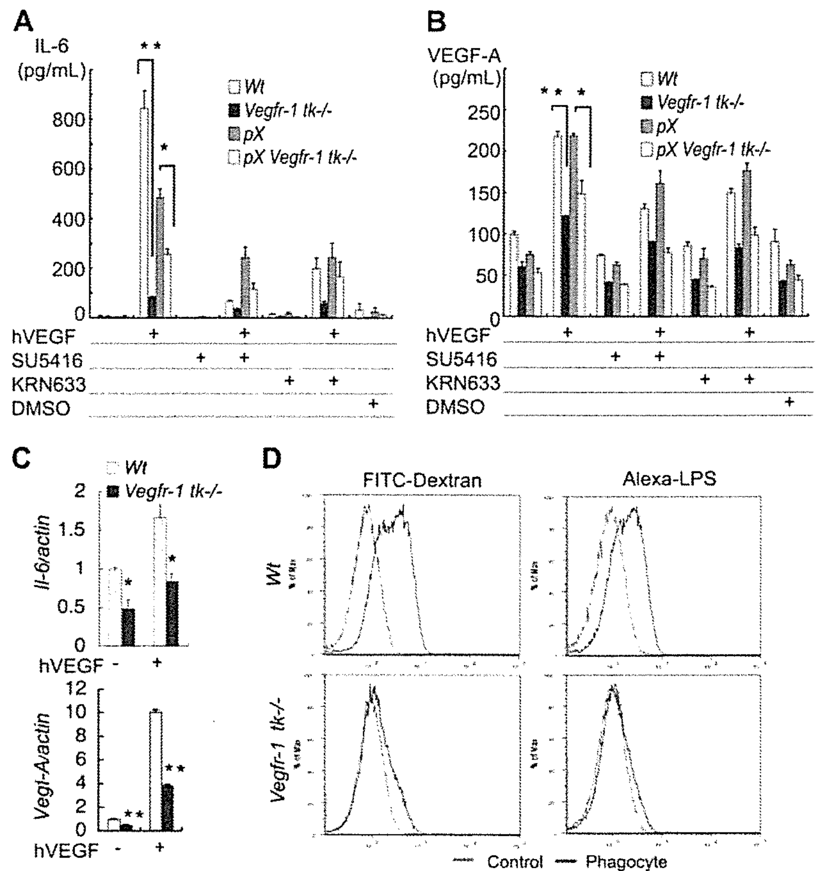

Figure 4. Cytokine secretion and phagocytosis are attenuated in the macrophages in *Vegfr-1 tk*$^{-/-}$ mice. (A-B) Mouse peritoneal macrophages were stimulated with hVEGF-A (100 ng/mL), and then levels of cytokines (IL-6 and VEGF-A) secreted into the medium were measured by ELISA after a 48-hour incubation. (A) IL-6 was secreted in response to hVEGF-A, and this secretion was partially suppressed by VEGFR inhibitors, SU5416 and KRN633. Secretion of IL-6 from *Vegfr-1 tk*$^{-/-}$ macrophages was low compared with that from the wild-type macrophages. (B) Mouse VEGF-A (mVEGF-A) was secreted from macrophages in the absence of hVEGF-A, and the secretion increased on stimulation with exogenous hVEGF-A. The secretion of mVEGF-A was partially suppressed by VEGFR inhibitors. The secretion from *Vegfr-1 tk*$^{-/-}$ macrophages was about half that from wild-type macrophages. Results represent the mean ± SEM from 2 to 3 experiments. (C) The mRNA expression of *Il-6* and *Vegf-A* on treatment with hVEGF-A was examined by real-time RT-PCR analysis. *Il-6* is weakly expressed in *Vegfr-1 tk*$^{-/-}$ macrophages. *Vegf-A* expression in *Vegfr-1 tk*$^{-/-}$ macrophages is about half that in the wild-type. (D) Macrophages derived from wild-type BM cells in cultures phagocytized dextran and LPS (upper row). On the other hand, macrophages from *Vegfr-1 tk*$^{-/-}$ BM did not show strong phagocytosis (lower row). Results are representative of at least 3 independent experiments. The data represent the mean ± SEM. *$P < .05$, **$P < .01$; wild-type versus *Vegfr-1 tk*$^{-/-}$ macrophages.

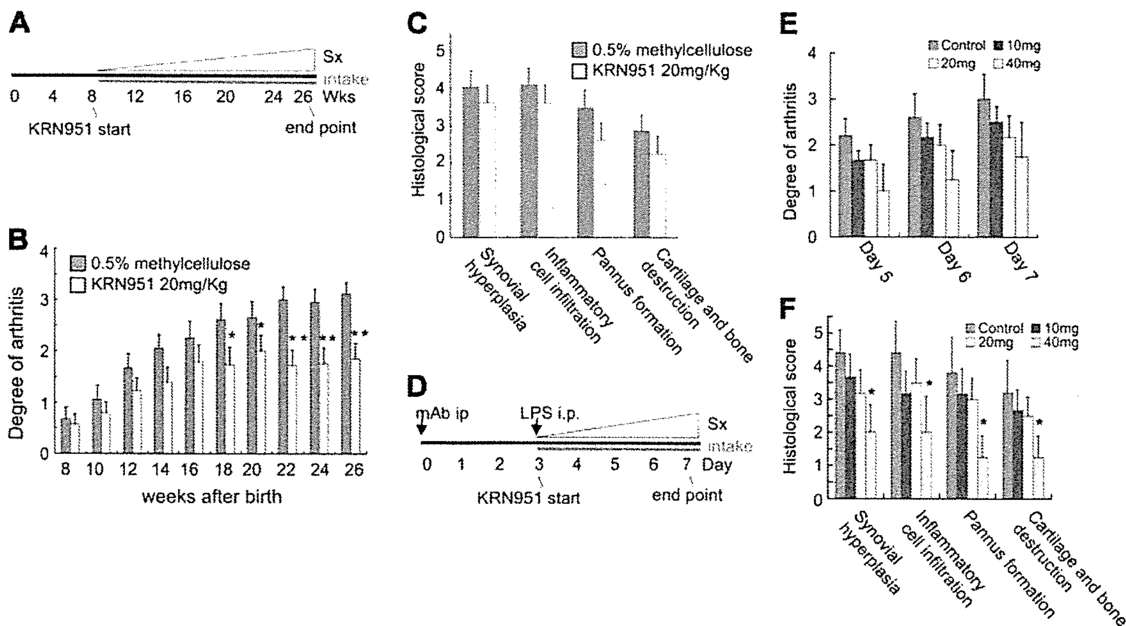

Figure 5. A VEGFR TK inhibitor, KRN951, suppressed the progression of *pX*-induced chronic and collagen-antibody–induced acute arthritis. (A) Experimental design for the treatment of mice with *pX*-induced chronic arthritis with a VEGFR inhibitor, KRN951. The VEGFR inhibitor was orally administered from 8 to 26 weeks of age (5 d/wk). (B) Clinical grades of arthritis gradually increased with age. The KRN951-administered group showed a reduction in the progression of arthritis compared with the untreated group. The data represent the mean ± SEM. *$P < .05$, **$P < .01$; KRN951-treated group versus control. (C) The scores of histologic findings in the treated group were also decreased (statistically not significant). (D) Experimental design for the treatment of mice with collagen-antibody–induced acute arthritis. Anticollagen-antibody was injected into the peritoneum of mice, followed by a peritoneal injection of LPS after 3 days. The administration of KRN951 started at day 3 and ended at day 7. (E-F) Clinical grade and histologic score of acute arthritis decreased in a KRN951 dose–dependent manner. The data represent the mean ± SEM. *$P < .05$; 40 mg/kg/d versus control. Sx indicates symptom.

could block the TK of VEGFR1 and VEGFR2 in vivo (K.N. and M.S., unpublished data, April 2006).

The administration of KRN951 in the acute model also reduced the progression of the symptoms of arthritis in a dose-dependent manner (P = .142 to .227 on day 5 to day 7. All values are 40 mg/kg/d versus control) (Figure 5E). KRN951 is a pan-VEGFR inhibitor; however, the arthritic symptoms and histologic abnormalities with KRN951 were as mild as those of *pX Vegfr-1 tk*–deficient mice. Taken together, these results suggest that VEGFR TKs, particularly VEGFR-1, contribute to the progression of arthritis.

VEGFR-1 is closely associated with the proliferation/differentiation of hematopoietic cells but not the number of BM hematopoietic stem cells

Another hallmark of hematopoietic activity is the capacity for colonies to form BMMNCs in vitro.[40] The colony-forming ability of *Vegfr-1* $tk^{-/-}$ BMMNCs was reduced to about 70% of that of wild-type BMMNCs (P = .013), and all the progenitors including erythroid colonies, myeloid colonies, and more immature mixed colonies were equally affected (P = .002, .091, and .021, respectively) (Figure 6A-B).

These results suggest at least 2 possibilities: a decrease in the activity of BM hematopoietic stem cells (HSCs) or a decrease in the number of HSCs in *Vegfr-1* $tk^{-/-}$ BM. To distinguish between these possibilities, we examined the number of HSCs by FACS analysis. Numbers of Sca-1$^+$ and CD34$^+$ cells corresponding to HSCs among BMMNCs were almost the same between wild-type and *Vegfr-1* $tk^{-/-}$ mice (Figure 6C). Therefore, a deficiency of VEGFR-1 signaling may reduce the proliferation of HSCs but not the number of these cells in BM.

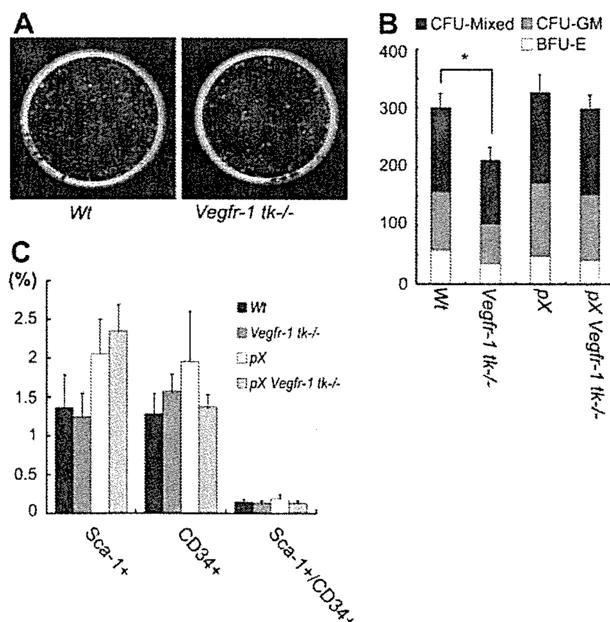

Figure 6. VEGFR-1 is associated with the proliferation of hematopoietic cells but not the number of BM HSCs. (A-B) The number of colony-forming units (CFU) in *Vegfr-1* $tk^{-/-}$ was decreased in all progenitor cells (BFU-E, CFU-GM, CFU-mixed) compared with that in wild-type mice (P = .013) (A). Each progenitor cell also showed a decrease in the number of colonies (P = .002 in BFU-E, .091 in CFU-GM, and .021 in CFU-mixed). Data represent the mean ± SEM for 3 mice. $^*P < .05$; wild-type BM versus *Vegfr-1* $tk^{-/-}$ BM (B). (C) The number of HSCs (Sca-1$^+$ and CD34$^+$ cells) in BM was not influenced by *Vegfr-1 tk* deficiency. Percentages of HSCs among BMMNCs were analyzed by flow cytometer. Results represent the mean ± SEM for 3 mice.

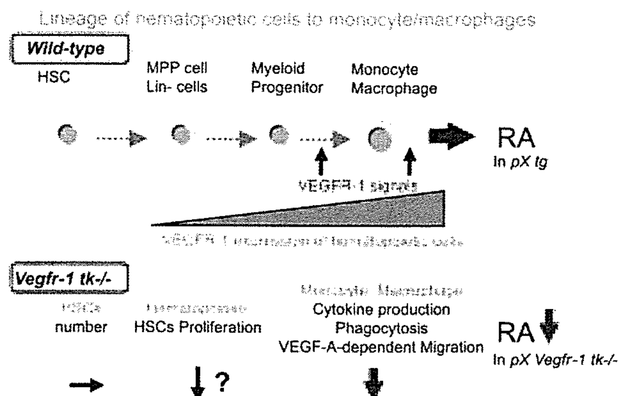

Figure 7. VEGFR-1 TK signaling is involved in arthritis by modulating hematopoiesis and promoting the differentiation of monocytes/macrophages. A schematic model of the VEGFR-1 TK signals associated with arthritis. (Top) Immature monocytes/macrophages derived from BM hematopoietic cells differentiate and migrate into the circulation. VEGFR-1 is expressed in monocyte/macrophage lineages. VEGFR-1 signals mobilize inflammatory cells to the peripheral tissues and RA joints and stimulate secretion of inflammatory cytokines to promote RA. (Bottom) VEGFR-1 signal–deficient macrophages show suppressed cytokine secretion, phagocytosis, and VEGF-dependent migration, resulting in a decrease in RA.

Discussion

In this study, we have shown that VEGFR-1 TK signals play a significant role in the progression of RA in murine models of both chronic and acute arthritis. Furthermore, the involvement of VEGFR-1 signals is considered to be gene-dosage dependent because the clinical and histologic scores of RA in *Vegfr-1* $tk^{+/-}$ heterozygous *pX* mice were between those of wild-type *pX* and *Vegfr-1* $tk^{-/-}$ mice. Several functions of macrophages such as the secretion of IL-6 and VEGF-A, phagocytosis, and VEGF-A–dependent migration were clearly suppressed in *Vegfr-1* $tk^{-/-}$ mice. In addition, the proliferation of HSCs decreased about 30% in the in vitro assay in these mice. These results suggest that the kinase activity of VEGFR-1 is important in a variety of steps during the progression of pathological inflammatory diseases such as RA (Figure 7).

Our results raise the question of which receptor for VEGFs, VEGFR-1 or VEGFR-2, is tightly linked to RA. The TK of VEGFR-2 appears to be essential for the maintenance of blood vessel networks in adulthood[4,15,20,41-44]; thus, *Vegfr-2* tk^- mice, similar to the *Vegfr-1* $tk^{-/-}$ mice in this study, are not available. However, the suppressive effect of *Vegfr-1 tk* deficiency on the RA model and that of the treatment with the pan-VEGFR kinase inhibitor KRN951 were similar (Figures 2 and 5A), suggesting that VEGFR-1 signaling is more strongly related to the progression of RA than VEGFR-2 signaling. In addition, the amount of newly formed capillary vessels in the pannus did not differ significantly between *pX Vegfr-1* $tk^{+/+}$ and *pX Vegfr-1* $tk^{-/-}$ mice. These results imply that inflammatory responses are more closely associated with VEGFR-1 than VEGFR-2. Consistent with these findings, Luttun et al[22] found that, using blocking antibodies against mouse VEGFR-1 or VEGFR-2, treatment with anti–VEGFR-1 Ab more efficiently suppressed an adjuvant-induced inflammatory arthritis than did treatment with anti–VEGFR-2 Ab. Furthermore, De Bandt et al[45] recently reported that VEGFR-1 is involved in a model of chronic arthritis in which the KRN/NOD ($\alpha v\beta 6$ T-cell receptor [TCR] transgene)/nonobese diabetic) mice were used for the induction of inflammation. Their model system is different from ours; therefore, results obtained with several independent animal